

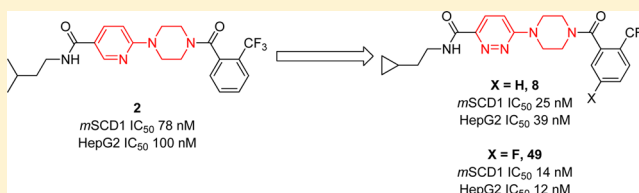
Discovery of Piperazin-1-ylpyridazine-Based Potent and Selective Stearoyl-CoA Desaturase-1 Inhibitors for the Treatment of Obesity and Metabolic Syndrome

Zaihui Zhang,[†] Shaoyi Sun,[†] Vishnumurthy Kodumuru,[†] Duanjie Hou,[†] Shifeng Liu,[†] Nagasree Chakka,[†] Serguei Sviridov,[†] Sultan Chowdhury,[†] David G. McLaren,[†] Leslie G. Ratkay,[†] Kuldip Khakh,[†] Xing Cheng,[†] Heinz W. Gschwend,[‡] Rajender Kamboj,[†] Jianmin Fu,[†] and Michael D. Winther^{*,†}

[†]Xenon Pharmaceuticals, Inc., 3650 Gilmore Way, Burnaby, BC V5G 4W8 Canada

[‡]Consultant, 161 Meadowcroft Way, Santa Rosa, California 95403, United States

ABSTRACT: Stearoyl-CoA desaturase-1 (SCD1) catalyzes de novo synthesis of monounsaturated fatty acids from saturated fatty acids. Studies have demonstrated that rodents lacking a functional SCD1 gene have an improved metabolic profile, including reduced weight gain, lower triglycerides, and improved insulin response. In this study, we discovered a series of piperazinylpyridazine-based highly potent, selective, and orally bioavailable compounds. Particularly, compound **49** (XEN103) was highly active in vitro (*m*SCD1 IC₅₀ = 14 nM and HepG2 IC₅₀ = 12 nM) and efficacious in vivo (ED₅₀ = 0.8 mg/kg). It also demonstrated striking reduction of weight gain in a rodent model. Our findings with small-molecule SCD1 inhibitors confirm the importance of this target in metabolic regulation, describe novel models for assessing SCD1 inhibitors for efficacy and tolerability and demonstrate an opportunity to develop a novel therapy for metabolic disease.



INTRODUCTION

Obesity and type 2 diabetes are emerging as two major global health problems of the 21st century. Evidence published over the past decade has shown that abnormal lipid metabolism is closely related to occurrence of metabolic syndrome, obesity, type 2 diabetes, and dyslipidemia.¹ One potential target for treatment of these diseases, which has recently received great attention in the scientific community, is stearoyl-CoA desaturase-1 (SCD1, commonly known as delta-9 desaturase, D9D).² SCD1 catalyzes de novo synthesis of monounsaturated fatty acids (MUFA) from saturated fatty acids by introduction of a cis double bond between carbons 9 and 10 positions of stearic acid and palmitic acid. The products, mainly oleate and palmitoleate, are key substrates for the synthesis of triglycerides, wax esters, cholesterol esters, and phospholipids.³ SCD1 is the major isoform present in lipogenic tissues (including liver and adipose tissues) in rodents and humans and functions as a key regulator of lipid and carbohydrate metabolism. SCD1-deficient mice have been shown to be lean and hypermetabolic.⁴ In the leptin-deficient model for obesity (*ob/ob*), mice with an inactive SCD1 gene were significantly less obese than the *ob/ob* controls and had markedly increased energy expenditure; in addition, these mice had histologically normal livers with significantly reduced triglyceride storage and very-low-density lipoprotein (VLDL) production.⁴ The data support a model in which SCD1 deficiency is associated with an activation of lipid oxidation and reduction of triglyceride synthesis and storage.^{5–7} Genetic models also show significant skin and eye effects arising from diminished SCD1 activity, an effect that needs to be

avoided in developing systemically administered compounds. The beneficial phenotypes seen in these genetic models are also observed in high fat diet-induced obese (DIO) mice treated with antisense oligonucleotides (ASOs) directed toward SCD1.^{8,9} In humans, a similar role for SCD1 can be postulated because elevated SCD1 activity positively correlates with high triglyceride levels in familial hypertriglyceridemia subjects,¹⁰ increased body mass index (BMI), and high plasma insulin levels.¹¹ Therefore, compounds that inhibit SCD1 may hold significant therapeutic potential for the treatment of obesity, type 2 diabetes, and other metabolic disorders.

No drug-like, selective SCD1 inhibitors were reported until we published a series of patent applications in 2005.^{12–16} These selective SCD inhibitors demonstrated that SCD1 activity could be potently inhibited by small drug-like molecules. Since then, a number of small-molecule SCD1 inhibitors have been reported.^{17–31} Our program targeting the discovery of small-molecule SCD1 inhibitors for the treatment of obesity and metabolic syndrome started with a high throughput screening campaign that identified a number of pyridin-2-ylpiperazine compounds with micromolar activity against mouse SCD1. Compound **1** (Figure 1) was the most potent identified from the library screen, with *m*SCD IC₅₀ of 5.1 μM. The initial hit-to-lead effort was focused on developing the SAR of this pyridin-2-ylpiperazine scaffold and a focused compound library of 588 compounds (Figure 1) was initially synthesized.^{32,33}

Received: November 9, 2012

Published: December 17, 2012



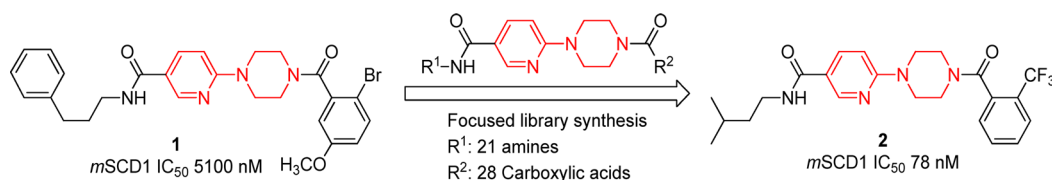


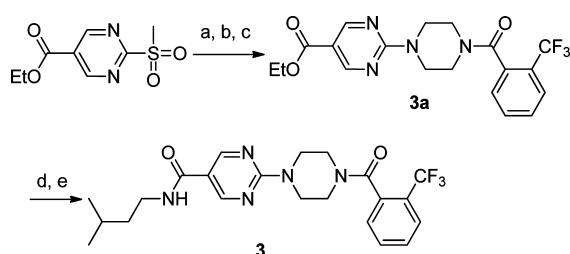
Figure 1. The structure of HTS hit (**1**) and the hit-to-lead process to identify compound **2** for lead optimization.

Several preferred amine (R^1) and carboxylic acids (R^2) were identified, and compound **2** emerged as the most potent with *m*SCD IC_{50} of 78 nM (Figure 1). Herein, we report on our lead optimization efforts toward compound **2**, which led to the discovery of a novel, potent, selective, and orally bioavailable piperazinylpyridazine inhibitor **49** (XEN103). The in vitro potency and in vivo efficacy will also be reported herein.

CHEMISTRY

2-(Piperazin-1-yl)pyrimidine analogue **3** (Scheme 1) was synthesized starting from ethyl 2-(methylsulfonyl)pyrimidine-

Scheme 1^a



^aReagents and conditions: (a) *tert*-butyl piperazine-1-carboxylate, DIPEA, 1,4-dioxane, 100 °C, 13 h; (b) TFA, DCM, rt, overnight; (c) 2-(trifluoromethyl)benzoyl chloride, DIPEA, DCM, 0 °C to rt, 6 h; (d) LiOH, THF/MeOH, H₂O, rt, 24 h; (e) isoamylamine, HOBt, EDCI, DIPEA, DCM, rt, 15 h.

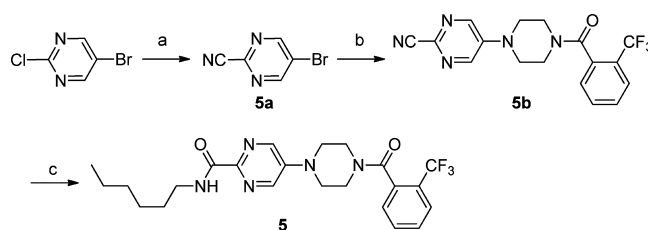
5-carboxylate. Under nucleophilic substitution reaction conditions, the methylsulfonyl group was replaced by *tert*-butyl piperazine-1-carboxylate. The BOC protecting group was removed with trifluoroacetic acid to afford the 2-(piperazin-1-yl)pyrimidine core structure. Amide formation with 2-(trifluoromethyl)benzoyl chloride yielded the ester intermediate **3a**. Ester saponification and amide formation between the carboxylic acid and isoamylamine yielded the final product **3**.

For the synthesis of 5-(piperazin-1-yl)pyrazine analogue **4** as outlined in Scheme 2, the sequence started from the amide formation between *tert*-butyl piperazine-1-carboxylate and 2-

(trifluoromethyl)benzoyl chloride, followed by the treatment with trifluoroacetic acid to afford piperazin-1-yl(2-(trifluoromethyl)phenyl)methanone **4a**. Replacement of the chloro group on methyl 5-chloropyrazine-2-carboxylate with compound **4a** via nucleophilic substitution generated the ester intermediate which was subjected to base hydrolysis to afford carboxylic acid **4b**. The final compound **4** was obtained after the amide formation between **4b** and isoamylamine.

The 5-(piperazin-1-yl)pyrimidine analogue was obtained following Scheme 3. Starting from commercially available 5-

Scheme 3^a

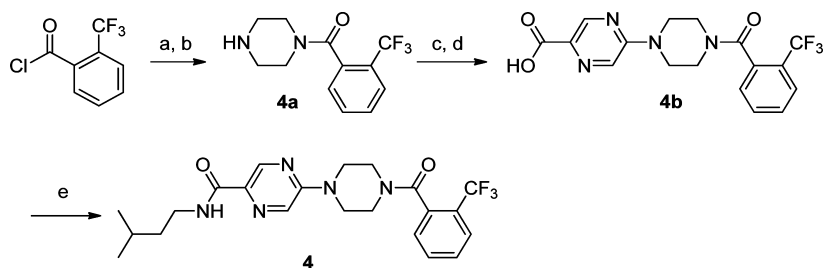


^aReagents and conditions: (a) NaCN, 0.15 equiv DABCO, H₂O/DMSO (1/1), rt, 2 h; (b) **4a**, Cs₂CO₃, NMP (0.25 M), 80 °C; (c) *n*-hexylamine, RuCl₂(PPh₃)₃, 1,2-dimethoxyethane, 160 °C.

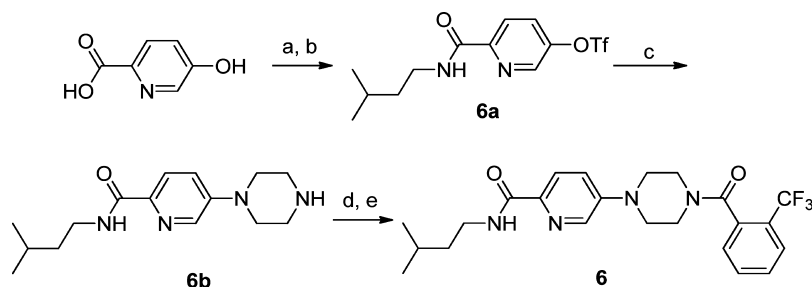
bromo-2-chloropyrimidine, replacement of the chloro group by a nitrile group was achieved in the presence of catalytic DABCO to generate compound **5a**. Under nucleophilic substitution reaction conditions, the bromo group of **5a** was replaced by compound **4a** to afford nitrile compound **5b**. Treatment of nitrile compound **5b** with *n*-hexylamine under ruthenium catalyzed amidation conditions,³⁴ afforded the desired product **5**.

For the synthesis of pyridine-3-ylpiperazine analogue **6** (Scheme 4), 5-hydroxypicolinic acid was treated with isoamylamine under the amide formation conditions, followed by the treatment with triflate anhydride to afford compound **6a**. Under palladium catalyzed coupling reaction conditions, the triflate group was replaced by *tert*-butyl piperazine-1-carboxylate and subsequent removal of BOC group with TFA generated

Scheme 2^a



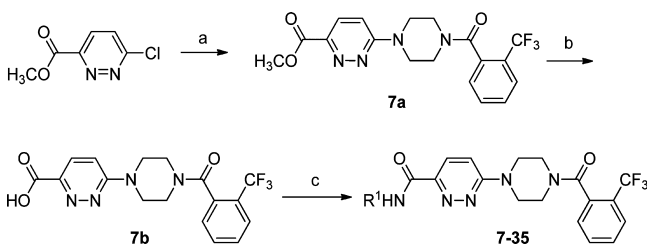
^aReagents and conditions: (a) *tert*-butyl piperazine-1-carboxylate, DIPEA, DCM; (b) 15% TFA, DCM, 1 h; (c) methyl 5-chloropyrazine-2-carboxylate, DBU, Bu₄NI, DMF, 80 °C, 70 h; (d) LiOH, MeOH/H₂O, 19 h; (e) isoamylamine, EDCI, HOBt, DIPEA, DCM, 18 h.

Scheme 4^a

^aReagents and conditions: (a) isoamylamine, HOBT, EDCI, DIPEA, DCM, rt, 23 h; (b) Trf_2O , pyridine, 0 °C to rt, 25 h; (c) *tert*-butyl piperazine-1-carboxylate, $\text{Pd}(\text{OAc})_2$, BINAP, DIPEA, DCM, 98 °C, 23 h; (d) TFA, DCM, rt, 15 h; (e) 2-(trifluoromethyl)benzoyl chloride, DIPEA, DCM, 0 °C to rt, 5 h.

compound **6b**. The amide formation between **6b** and 2-(trifluoromethyl)benzoyl chloride afforded the desired product **6**.

The piperazin-1-ylpyridazine analogues with different R^1 groups were synthesized following Scheme 5. Starting from

Scheme 5. General Synthetic Route for Piperazin-1-ylpyridazine Libraries with Different R^1 ^a

^aReagents and conditions: (a) piperazin-1-yl(2-(trifluoromethyl)phenyl)methanone **4a**, K_2CO_3 , Bu_4NI , 1,4-dioxane, reflux, 24 h; (b) LiOH , $\text{THF}/\text{H}_2\text{O}$, rt, 6 h; (c) thionyl chloride, DMF, reflux, 18 h; R^1NH_2 , Et_3N , DCM, rt, 4 h.

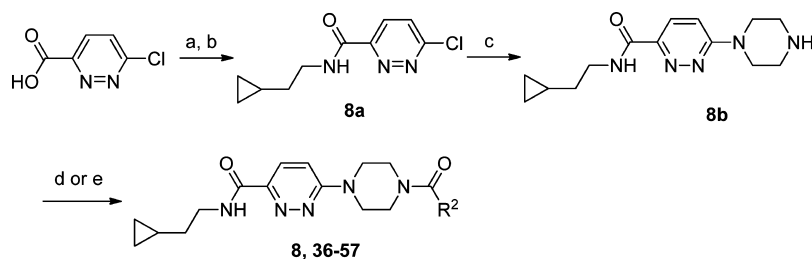
methyl 6-chloropyridazine-3-carboxylate, replacement of the chloro group with compound piperazin-1-yl(2-(trifluoromethyl)phenyl)methanone **4a** via nucleophilic substitution afforded the intermediate **7a**, which was hydrolyzed under basic conditions to generate the carboxylic acid **7b**. The amide formation between the acid chloride of **7b** and appropriate amines afforded the final compounds **7–35**.

The piperazin-1-ylpyridazine analogues with different R^2 groups were synthesized following Scheme 6. 6-Chloropyridazine-3-carboxylic acid was converted to the acid chloride by the treatment with thionyl chloride, followed by the reaction

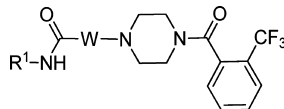
with 2-cyclopropylethylamine to generate compound **8a**. Under nucleophilic substitution reaction conditions, the chloro group of **8a** was replaced by piperazine to afford compound **8b**. Amide formation between **8b** and appropriate acid chlorides or appropriate carboxylic acids generated final compounds **8** and **36–57**.

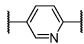
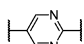
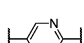
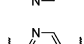
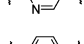
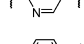
RESULTS AND DISCUSSION

The potency of all compounds was assessed in a series of assays beginning with a mouse liver microsomal assay as the primary biochemical assay. Compounds showing significant inhibition in this assay were then advanced for further characterization in a human liver hepatocellular carcinoma (HepG2) cell-based assay. In the mouse liver microsomal assay, the SCD1 activity was determined by measuring decreased production of tritiated water released from the (9,10- ^3H)-labeled stearoyl coenzyme A substrate. In the human HepG2 cell-based assay, SCD1 activity was assessed by determination of the amount of ^{14}C -oleic acid product formed from ^{14}C stearate substrate. The activity against desaturase-5 and desaturase-6 was also evaluated to determine the desaturase selectivity. We initiated our structure–activity relationship (SAR) exploration using compound **2** as the starting point. Because of the novelty concerns associated with the original pyridin-2-ylpiperazine core structure, our initial analogue efforts were focused on the replacement of the pyridin-2-yl moiety with alternative six-membered nitrogen-containing heterocycles. The results summarized in Table 1 demonstrated that analogues with pyrimidine (compounds **3** and **5**) and pyrazine (compound **4**) replacements had dramatically decreased the SCD1 activity. The pyridin-3-yl replacement (compound **6**) retained activity in mouse liver microsomal assay, but it was more than 24-fold less potent in human HepG2 assay. The best results were obtained with the

Scheme 6. General Synthetic Route for Piperazin-1-ylpyridazine Libraries with Different R^2 Groups^a

^aReagents and conditions: (a) thionyl chloride, DMF (catalytic amount), chloroform, reflux, 1 h; (b) 2-cyclopropylethylamine, Et_3N , 0 °C to rt, 30 min.; (c) piperazine, acetonitrile, reflux, 2 h; (d) R^2COCl , Et_3N , DCM, 0 °C to rt, 1 h; (e) R^2COOH , HOBT, EDCI, DIPEA, DCM, rt, overnight.

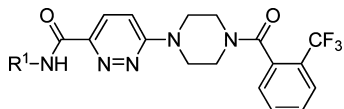
Table 1. SAR of Analogues with the Replacement of Pyridine-2-yl Moiety


Compound	R ¹	W	mSCD1 IC ₅₀ (nM) ^a	HepG2 IC ₅₀ (nM) ^a
2	isoamyl		78	100
3	isoamyl		>10000	ND ^b
4	isoamyl		>10000	ND
5	n-hexyl		1200	6400
6	isoamyl		220	2400
7	isoamyl		26	37

^aIC₅₀ data presented are means of $n \geq 2$. ^bND = not determined.

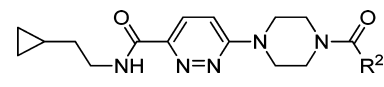
pyridazine replacement (compound 7), which improved the potency by about 3-fold in both assays. Moreover, this compound possessed reasonable drug-like properties such as minimal or no detectable CYP inhibitory activity (<50% inhibition at 10 μ M for CYP3A4, 2C9, 2C19, and 2D6), reasonable metabolic stability (57% remaining after 30 min incubation in rat liver microsomes), good cell permeability (in Caco-2 cells, Papp(a to b) 25×10^{-6} cm/s), and moderate protein binding (78% bound). In addition, pyridazine compound 7 demonstrated a robust in vivo pharmacodynamic response (PD) inhibiting rat liver SCD1 activity by about 40% at 4 h post final dose after two days of once daily dosing intraperitoneally (ip) at 15 mg/kg.

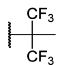
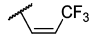
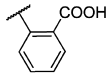
Encouraged by the discovery of the pyridazine replacement, our optimization efforts were then focused on the piperazinylpyridazine template to improve the SCD1 potency, pharmaceutical properties, and more importantly, in vivo activity. We first kept the right-hand side of the molecule constant using the 2-trifluoromethylbenzoyl group and varied the left-hand side amide with diverse amines. The results are summarized in Table 2. It was clearly demonstrated that a variety of structural modifications at R¹ were well tolerated. For cycloalkylalkyl groups, the length of the linker between the

Table 2. SAR and Properties of Piperazinylpyridazine Analogues with Different R¹ Groups


compd	R ¹	mSCD1 IC ₅₀ (nM) ^a	HepG2 IC ₅₀ (nM) ^a	RLM stability ^b	cell permeability ^c
8	cyclopropylethyl	25	39	76	24/22
9	cyclopropylmethyl	8690	ND ^d	ND	ND
10	3-cyclopropylpropyl	34	10	63	32/30
11	4-cyclopropylbutyl	10	100	42	13/17
12	3-hydroxy-3-methylbutyl	10000	ND	ND	ND
13	2-ethoxyethyl	1250	ND	ND	ND
14	pentyl	25	28	49	22/22
15	hexyl	21	24	14	20/18
16	heptyl	18	1100	ND	ND
17	4-chlorophenyl	7	3	65	2/2
18	phenyl	83	125	9	13/10
19	benzyl	6	41	97	34/34
20	phenethyl	18	18	56	16/15
21	3-phenylpropyl	69	125	ND	ND
22	2-phenylpropyl	150	660	ND	ND
23	(R)-2-hydroxy-2-phenylethyl	19	15	92	22/28
24	(S)-2-hydroxy-2-phenylethyl	25	60	82	23/29
25	2-oxo-2-phenylethyl	42	23	63	22/23
26	pyridine-2-yl	1405	ND	ND	ND
27	pyridine-2-ylmethyl	352	ND	ND	ND
28	1H-benzo[d]imidazol-2-yl	11	70	92	25/23
29	(5-methylpyrazin-2-yl)methyl	33	2249	ND	ND
30	thiazol-2-ylmethyl	32	325	79	29/29
31	oxazol-4-ylmethyl	272	ND	ND	ND
32	oxazol-2-ylmethyl	500	ND	ND	ND
33	(5-methylfuran-2-yl)methyl	15	68	37	25/23
34	(5-(trifluoromethyl)furan-2-yl)methyl	31	124	78	18/18
35	(1H-pyrazol-3-yl)methyl	>1000	ND	ND	ND

^aIC₅₀ data presented are means of $n \geq 2$. ^bPercentage of parent compound remaining analyzed by LC/MS/MS after a 30 min incubation period with rat liver microsomes. ^cPermeability was determined using Caco-2 cells. The data were expressed as Papp(a to b) ($\times 10^{-6}$ cm/s)/Papp(b to a) ($\times 10^{-6}$ cm/s). ^dND = not determined

Table 3. SAR and Properties of Analogues of Piperazinylpyridazine with Different R² Groups


Compound	R ²	<i>m</i> SCD1 IC ₅₀ (μM) ^a	HepG2 IC ₅₀ (μM) ^a	RLM stability ^b	Permeability ^c
8	2-trifluoromethylphenyl	25	39	76	24 / 22
36		113	119	ND	ND
37		>10000	ND	ND	ND
38	2-trifluoromethylcyclopropyl	>1000	ND	ND	ND
39	2-methylcyclohexyl	680	ND	ND	ND
40	2-trifluoromethylfuran-3-yl	260	290	ND	ND
41	2-chloro-4-trifluoromethylpyrimidin-5-yl	321	5870	ND	ND
42	5-methyl-2-trifluoromethylfuran-3-yl	72	62	36	21 / 21
43	2-cyanophenyl	>1000	ND	ND	ND
44		>10000	ND	ND	ND
45	2-fluorophenyl	>1000	ND	ND	ND
46	2-(dimethylamino)phenyl	920	ND	ND	ND
47	2-chloro-5-(dimethylamino)phenyl	>10000	ND	ND	ND
48	2-chloro-5-fluorophenyl	62	192	66	28 / 29
49	5-fluoro-2-(trifluoromethyl)phenyl	14	12	74	30 / 30
50	5-fluoro-2-methoxyphenyl	710	ND	ND	ND
51	5-chloro-2-trifluoromethylphenyl	12	18	69	32 / 30
52	2,5-dimethylphenyl	942	ND	ND	ND
53	2,5-difluorophenyl	3114	ND	ND	ND
54	2,5-dichlorophenyl	34	101	ND	ND
55	2,5-bis(trifluoromethyl)phenyl	149	ND	ND	ND
56	3-fluoro-2-trifluoromethylphenyl	58	66	72	20 / 26
57	4-fluoro-2-trifluoromethylphenyl	21	24	69	22 / 22

^aIC₅₀ data presented are means of $n \geq 2$. ^bPercentage of parent compound remaining analyzed by LC/MS/MS after a 30 min incubation period with rat liver microsomes. ^cPermeability was determined using Caco-2 cells. The data were expressed as Papp(a to b) ($\times 10^{-6}$ cm/s) / Papp(b to a) ($\times 10^{-6}$ cm/s). ^dND = not determined.

terminal cyclopropyl group and the amide was important for activity against SCD1. Cyclopropylmethyl compound **9** was 250–800-fold less potent than its counterparts, with a longer linker (compounds **8**, **10**, and **11**) in the mouse liver microsomal assay. A similar trend was observed with alkyl substituents (compounds **14**, **15**, and **16**). Incorporation of a hydroxyl group into the alkyl chain (compounds **12**) dramatically decreased the activity against SCD1 in mouse liver microsomal assay (IC₅₀ ~ 10 μM). The compound containing an oxygen heteroatom in the chain (compound **13**) was not well tolerated, and the activity was decreased by about

50-fold. Replacing the isoamyl group with a phenyl-containing group afforded good potency against SCD1 in both assays. However, the potency was dependent upon the chain length between the phenyl group and the amide. Compounds **18–21** were all quite potent against SCD1 in both assays, but compounds with a benzyl (**19**) and phenethyl (**20**) group were more potent than those compounds with a phenyl (**18**) and 3-phenylpropyl (**21**) group. The optimal chain length between the phenyl group and the amide was found to be 2 or 3 carbon atoms. The chlorophenyl compound (**17**) also displayed good potency in both assays, however, its cell permeability was poor.

Methyl substitution on the alkyl linker resulted in a decrease in activity as demonstrated by compound 22. Incorporation of a hydroxyl group (compound 23 (R enantiomer) and compound 24 (S enantiomer)) or a carbonyl group (compound 25) into the linker was tolerated. Introduction of a pyridine-2-yl led to decreased activity (compounds 26 and 27). Similar results were obtained for pyridine-3-yl and pyridine-4-yl compounds (data not shown). The 5-methylpyrazin-2-ylmethyl compound 29 retained activity in the mouse liver microsomal assay, however, the cell-based HepG2 activity was decreased by more than 60-fold. In contrast, the benzimidazol-2-yl compound 28 retained good potency in both assays. In a series of five-membered heterocycles represented by compounds 30–35, furan and thiazole compounds retained good activity and oxazole compounds had modest activity, while pyrazole compound were much less active. Compounds that demonstrated potency in cell-based assay were also evaluated for their selectivity against delta-5 and delta-6 desaturases, and none of the compounds tested in these assays demonstrated significant inhibition of these two desaturases at 10 μ M (data not shown).

To further investigate the SAR of the right-hand side of the molecule (R^2), the 2-cyclopropylethyl group was kept unchanged and R^2 was varied (Table 3). In contrast to the left-hand side of the molecule, the tolerance for structural modifications was much more stringent for R^2 . A dramatic decrease in activity against SCD1 in the mouse liver microsomal assay was observed with alkyl compounds 36–37, cycloalkyl compounds 38–39, and heteroaryl compounds 40–41, however, the 5-methyl-2-(trifluoromethyl)furan-3-yl analogue 42 retained good activity against SCD1 in both assays. Because replacing the 2-trifluoromethylphenyl group presented in compound 8 with the alkyl, cycloalkyl, and heteroaryl groups did not provide any advantages, we therefore returned to the original 2-trifluoromethylphenyl group to explore the substituent effects. When the 2-trifluoromethyl group was replaced by other electron-withdrawing groups, such as $-\text{CN}$ (43), $-\text{COOH}$ (44), $-\text{F}$ (45), or electron-donating groups such as $-\text{N}(\text{CH}_3)_2$ (46), $-\text{OCH}_3$ (50), and $-\text{CH}_3$ (52), the activity against SCD1 was decreased by 28- to 400-fold in the mouse liver microsomal assay. We explored the effect of disubstitution with a series of compounds, 47–57. Our findings, in general, support the notion that the presence of an electron-withdrawing group in addition to the trifluoromethyl group enhances the SCD1 inhibitory activity. For example, compound 49, containing an F group *para* to the trifluoromethyl group, demonstrated an enhanced activity by \sim 2–3-fold in both assays. Incorporation of an electron-donating group, such as the $-\text{N}(\text{CH}_3)_2$ group *para* to the 2-Cl group (47), resulted in decreased activity. The corresponding electron-withdrawing *para*-F compound (48) was 160-fold more potent than 47. From this work, the 2-trifluoromethylphenyl group was identified as the optimum group to achieve good potency, while an extra electron-withdrawing group on the phenyl ring further enhanced the activity. Compounds that demonstrated potency in cell-based assay were also tested for their selectivity against delta-5 and delta-6 desaturases, and the inhibition of these two desaturases was not significant at 10 μ M (data not shown).

Compounds with $\text{IC}_{50} < 100$ nM in cell-based assay were also evaluated in an acute rat pharmacodynamic (PD) model to determine the effect of these SCD1 inhibitors on the liver SCD1 activity. In these studies, Lewis rats were dosed with 1 mg/kg compound orally and then sacrificed 4 h after dosing.

The SCD1 activities of the liver microsomes obtained from these rats were determined, and the results are illustrated in Figure 2. Many of our SCD1 inhibitors showed robust effects in

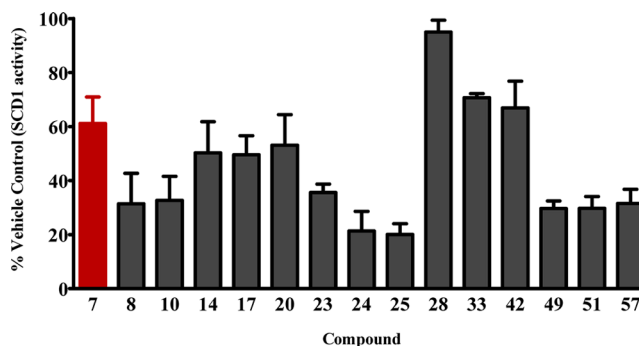


Figure 2. Effect of SCD1 inhibitors on rat liver SCD1 activity in rat PD model. Lewis rats were fed with high carbohydrate diet for one week before the study. The rats were fasted for 4 h prior to dosing. The rats ($n = 4$) were dosed orally with compound at 1 mg/kg dose in Tween 20 0.2%/CMC (1%) 99.8% formulation and sacrificed 4 h post dosing. The livers were harvested and homogenized. The activities of these liver microsomes were determined by the method as described in the Experimental Section. Compound 7 was dosed ip at 15 mg/kg for two days. Each bar represents the mean of at least four rats and the standard deviation from the mean.

this acute PD model as early as 4 h postdose. These results mark the first report on such an acute and robust effect of SCD1 inhibitors in vivo without using a radioactive label and thus demonstrate the utility of this rodent model for efficient in vivo compound screening. In comparison to the early compound 7, many compounds had dramatically improved PD effects. Compounds 8, 10, 24, 25, 49, 51, and 57 all decreased liver SCD1 activity by more than 60%. Although most compounds showed in vivo PD effects, the in vitro to in vivo activity correlation was poor. For example, compounds 28, 33, and 42 all had less than 100 nM potency in both in vitro assays, but their in vivo activities were $<30\%$ inhibition of rat liver SCD1 activity. Compound 17, which was the most potent compounds in vitro (<10 nM), had only moderate effects in the Lewis rat PD model (Figure 2). Possible explanations for the activity disconnect include differences in metabolic stability, permeability, PK profiles, and bioavailability.

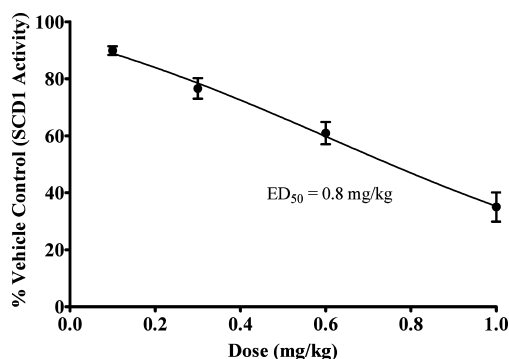
To better understand what drives the in vivo PD response, pharmacokinetic (PK) profiles were determined for several potent SCD1 inhibitors including 8, 25, 28, 49, and 51 (Table 4). All compounds shown below had similar metabolic stability in rat liver microsomes, however, their in vivo clearance rates were quite different. Compound 25 had very low clearance, a small volume of distribution, high plasma exposure, and good bioavailability. It demonstrated a profound PD effect in the rat PD model (Figure 2). Compound 28, on the other hand, demonstrated high clearance, very low plasma exposure, and reduced oral bioavailability, and a marginal PD effect was observed in vivo (Figure 2). Compounds 8, 49, and 51, which share structural similarity, possessed similar PK profiles and oral bioavailability and they all demonstrated a similarly profound PD effect in vivo (Figure 2). On the basis of the in vitro and in vivo activity, as well as overall drug-like properties, compound 49 was chosen for further in vivo testing to evaluate its effects on metabolic disease.

Table 4. Pharmacokinetic Parameters for SCD1 Inhibitors in Lewis Rats (3 mg/kg IV and 10 mg/kg PO Doses Unless Otherwise Stated)

compd	IV ^a				PO ^a			
	$t_{1/2}$ ^b	AUC ^c	V_{ss} ^d	Cl ^e	C_{max} ^f	T_{max} ^g	AUC ^h	F ⁱ
8 ^j	1.0	220	2.2	1.9	0.9	1.0	167	46
25	1.8	1238	0.7	0.28	1.9	3.3	1756	42
28 ^k	1.1	1.6	1.8	1.3	0.07	0.5	0.6	19
49 ^l	1.6	96.6	2.7	1.3	0.9	3.3	485	49
51	1.8	453	1.6	0.86	0.5	2.3	459	30

^aAverage of at least two rats for IV and three rats for PO per compound. ^bIntravenous half-life (h). ^cArea under the curve or total drug exposure after intravenous dosing from $t = 0$ to $t = \infty$ ($\mu\text{M}\cdot\text{h}$). ^dIntravenous volume of distribution at steady state (L/kg). ^eClearance after intravenous dosing ((L/h)/kg). ^fMaximum plasma concentration after oral dosing (μM). ^gTime from oral dosing to maximum plasma concentration (h). ^hArea under the curve or total drug exposure after oral dosing from $t = 0$ to $t = \infty$ ($\mu\text{M}\cdot\text{h}$). ⁱOral bioavailability (%). ^jPO dose 5 mg/kg. ^kDose: IV 1 mg/kg and PO 2 mg/kg. ^lIV dose 1 mg/kg.

Compound **49** was evaluated in the Lewis rat PD model in a dose responsive manner at doses ranging from 0.1 to 1 mg/kg (4 h post oral dosing sampling). The results illustrated in Figure 3 indicate a clear dose related reduction of liver SCD1 activity with an ED_{50} estimated as 0.8 mg/kg.

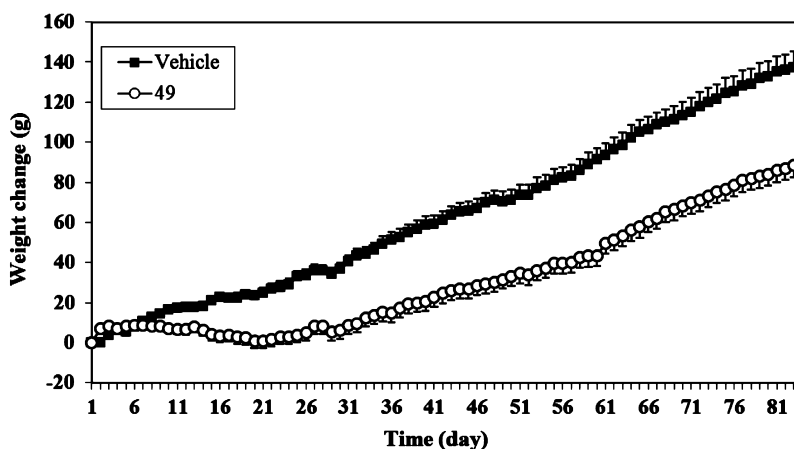
**Figure 3.** Dose response of **49** on inhibition of liver SCD1 activity 4 h after PO dosing in Lewis rats. Each bar represents the standard deviation from the mean of at least four rats.

To assess the impact of SCD1 inhibition by **49** on energy balance and weight maintenance, an in vivo study utilizing Zucker Fatty rats was conducted examining metabolic end points. The Zucker Fatty rats are obese, hyperphagic, hyperinsulinemia, and hypertriglyceridemia and show an age-dependent decreased energy expenditure.^{35,36} In this study, **49** was administered orally to the rats twice daily for 15 weeks. The effect of **49** on the following metabolic parameters was evaluated at the end of the study: body weight (at the end of 12 weeks), body fat mass using dual-energy X-ray absorptiometry (DEXA), metabolic rate, and resting oxygen consumption by indirect calorimetry.

Oral administration twice daily with 1 mg/kg **49** to 20-week-old Zucker Fatty rats resulted in a significant 36% reduction in the total body weight gained over a 12-week period when compared to the vehicle treated controls. The reduction in body weight gain was observed within the first week of the treatment and was maintained for the 12 weeks of measurement (Figure 4).

At the end of 15-week study, the rats were sacrificed and the epididymal, retroperitoneal, and mesenteric fat pads were collected and measured to provide the combined visceral fat weights. The **49** treatment group demonstrated a 24% reduction in combined visceral fat weight when compared to the vehicle control group (Figure 5A; $p < 0.001$). All three visceral fat pads measured were reduced in the **49** treatment group. In addition, dual energy X-ray absorptiometry (DEXA) measurements of bone mineral content (BMC), lean mass (LM), and fat mass (FM) in the thoracovisceral area of the carcasses were carried out. The **49** treatment group showed a 9% reduction in body fat percentage when compared to the vehicle control group (Figure 5A; $p = 0.002$). The fat mass was reduced by 20% in the **49** treatment group (Figure 5B; $p < 0.0001$). In contrast, lean mass and bone mineral content were not reduced (Figure 5B).

To confirm that the effects observed with **49** were due to SCD inhibition, plasma PD (as measured by desaturation index) was evaluated. The **49** treatment group demonstrated a significant reduction of C16 plasma DI by 73% and C18 plasma DI by 61%, respectively, when compared to vehicle control (Figure 6; $p < 0.001$).

**Figure 4.** Total body weight change during 12 weeks of treatment with **49**. Rats were weighed every day, and the change in weight from day zero was calculated for each rat. Each bar represents the mean of 24 rats and the standard error from the mean. **49** was administered orally twice daily at a dose of 1 mg/kg.

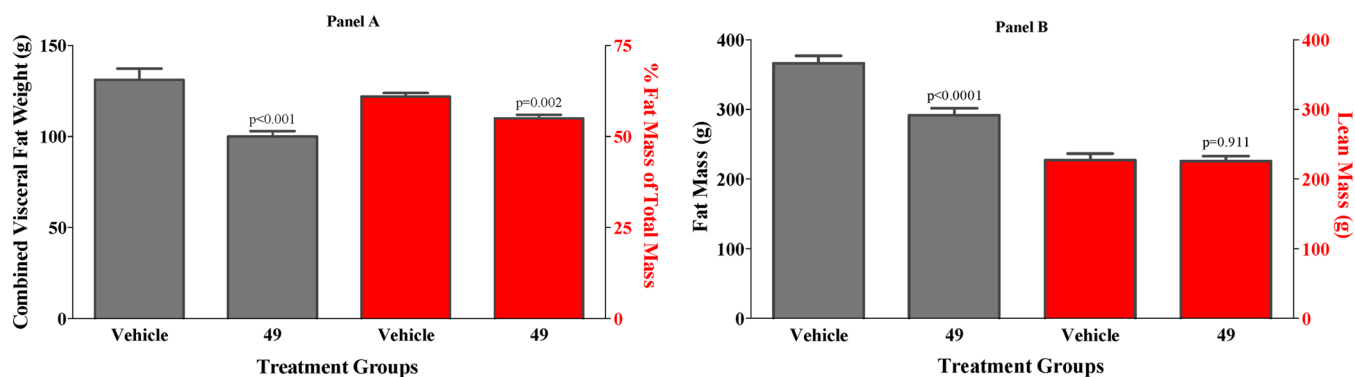


Figure 5. Effect of **49** on combined visceral fat weight and body fat mass (A) and on fat mass and lean mass (B) after 15 weeks oral administration of **49** at 1 mg/kg twice daily. The percentage of fat mass over the sum of BMC, LM, and FM was calculated to provide the fat %. Each bar represents the mean of 12 rats and the standard error from the mean.

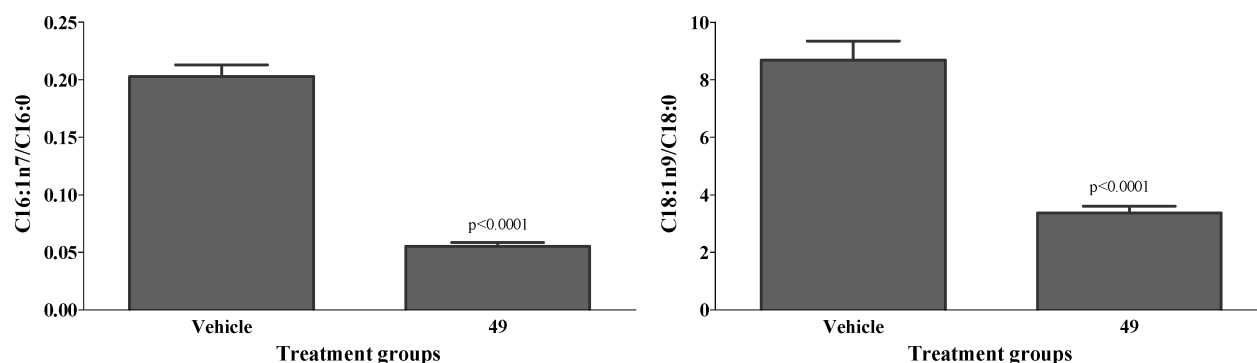


Figure 6. Plasma DI changes after a 15-week study of Zucker Fatty rats with **49**. Each bar represents the mean of 12 rats and the standard error from the mean. **49** was administered twice daily at a dose of 1 mg/kg.

To evaluate the potential mechanism-based side effect of a systemic SCD1 inhibitor, we also developed a clinical observation model. In this model, rats were administered orally once daily at a dose 20-fold of the efficacious dose determined by the rat PD model for 11 days. Rats were examined daily for general health and the specific observations on eyes and skin. Compounds with high systemic exposure manifested mechanism-based toxicity as early as day 3 of dosing as red eye and dry skin symptoms. This model provided us an efficient means to assess the mechanism-based toxicity of SCD1 inhibition.

CONCLUSIONS

We identified a series of piperazinyipyridazine-based highly potent, selective, and orally bioavailable SCD1 inhibitors. The SAR analysis demonstrated that the 2-trifluoromethylphenyl group was the optimal right-hand side group to achieve strong inhibitory activity against SCD1 activities in both mouse liver microsomal assay and cell-based HepG2 assay. In vivo studies demonstrated that a diverse set of piperazinyipyridazine compounds had an acute impact on the liver SCD1 activity within 4 h after a single oral dose. This investigation led us to identify a highly potent, selective, and efficacious SCD1 inhibitor: *N*-(2-Cyclopropylethyl)-6-(4-(5-fluoro-2-(trifluoromethyl)benzoyl)piperazin-1-yl)-pyridazine-3-carboxamide (**49**). Compound **49** demonstrated a very strong potency in liver SCD1 inhibition (ED_{50} = 0.8 mg/kg). This highly efficacious inhibition is likely due to a combination of strong enzymatic inhibitory activity (IC_{50} = 14 nM) and good oral bioavailability (F = 49%).

The in vivo study with Zucker Fatty rats with orally administration of **49** clearly demonstrated a significant reduction of total body weight gain, with a concordant decrease in visceral fat pad weight, without decreasing lean body mass. It clearly demonstrate that small-molecule inhibitors with favorable pharmacology are capable of recapitulating the improved metabolic parameters observed in the genetically SCD1 deficient animal. However, the systemic SCD1 inhibitors can also recapitulate other features observed in the SCD1 knockout mouse such as dry skin and dry eye side effects. Models were developed to assess the relative effects of SCD1 inhibitors on liver SCD1 (one of the sites of action associated with beneficial metabolic changes) and the eye and skin (adverse mechanism-based effects). The use of these models allows effective screening of compounds that have maximum effect in the liver yet do not appear to cause changes to eye and skin. Examination of **49** by topical administration on sebaceous glands as potential acne therapy will be reported in due course.

EXPERIMENTAL SECTION

General. All reagents were obtained from commercial sources and were either used as supplied or purified using reported methods. Melting points were determined on a Büchi hot-stage apparatus and are uncorrected. 1H NMR spectra were recorded on a Bruker Avance 300 spectrometer with chemical shifts (δ) reported in parts per million (ppm) relative to the residual signal of the deuterated solvent. 1H NMR data are tabulated in the following order: multiplicity (s, singlet; d, doublet; t, triplet; m, multiplet; br, broad), coupling constants in hertz, and number of protons. Mass spectra were obtained using a Waters 2795/ZQ LC/MS system (Waters Corporation, Milford, MA). HPLC analyses were performed at 25 °C on Agilent 1100 or 1200

systems (Agilent Technologies, Santa Clara, CA) using an EMD Chromolith SpeedROD RP-18e column (4.6 mm i.d. \times 50 mm length) (Merck KGaA, Darmstadt, Germany). The mobile phase consisted of a gradient of component "A" (0.1% v/v aqueous trifluoroacetic acid) and component "B" (acetonitrile) at a flow rate of 1 mL/min. The gradient program used was as follows: initial conditions 5% B, hold at 5% B for 1 min, linear ramp from 5% to 95% B over 5 min, 100% B for 3 min, return to initial conditions for 1 min. Peaks were detected at a wavelength of 254 nm with an Agilent photodiode array detector. All compounds reported herein exhibited spectral data consistent with their proposed structures and had HPLC purities in excess of 96% a/a. Chemical names were generated using ChemBioDraw version 12 by CambridgeSoft.

Ethyl 2-(4-(2-(trifluoromethyl)benzoyl)piperazin-1-yl)pyrimidine-5-carboxylate (3a). A mixture of ethyl 2-(methylsulfonyl)pyrimidine-5-carboxylate (33 mg, 0.14 mmol), *tert*-butyl piperazine-1-carboxylate (21 mg, 0.15 mmol), and DIPEA (26 μ L, 0.15 mmol) in 1,4-dioxane 4 mL was refluxed for 13 h and then concentrated in vacuo. The residue was washed with water (3 \times 10 mL) and dried in vacuo and dissolved in 15% TFA in DCM (2 mL). The mixture was stirred at room temperature overnight. The volatiles were removed in vacuo, and the residue was dissolved in DCM (4 mL), followed by the addition of DIPEA (122 μ L, 0.7 mmol) and 2-(trifluoromethyl)benzoyl chloride (22 μ L, 0.15 mmol) in DCM (3 mL) at 0 $^{\circ}$ C. The resulting solution was stirred at room temperature for 6 h, and EtOAc (40 mL) was added. The organic layer was separated and washed with brine, dried over anhydrous Na_2SO_4 , and concentrated. The residue was purified by column chromatography to afford **3a** as a colorless gum (45 mg, 78% yield). MS (ES+) m/z 409.3 (M + H) $^{+}$.

N-Isopentyl-2-(4-(2-(trifluoromethyl)benzoyl)piperazin-1-yl)pyrimidine-5-carboxamide (3). A solution of ethyl 2-(4-(2-(trifluoromethyl)benzoyl)piperazin-1-yl)pyrimidine-5-carboxylate **3a** (45 mg, 0.11 mmol) in a mixture of THF/MeOH/water (3:1:1, 5 mL) was stirred at room temperature for 24 h and concentrated. The residue was diluted with aqueous HCl solution and extracted with DCM (5 \times 20 mL). The combined organic layer was dried over anhydrous Na_2SO_4 and concentrated. The residue was dissolved in DCM (4 mL), followed by the addition of HOBt monohydrate (17 mg, 0.11 mmol), EDCI (21 mg, 0.11 mmol), DIPEA (38 μ L, 0.22 mmol), and isoamylamine (13 μ L, 0.11 mmol). The mixture was stirred at room temperature for 15 h and diluted with DCM (50 mL). The organic layer was washed with diluted HCl solution, brine, dried over anhydrous Na_2SO_4 , and concentrated. The residue was purified by column chromatography to afford **3** as a colorless gum (46 mg, 94% yield). ^1H NMR (300 MHz, CDCl_3) δ 8.68 (s, 2H), 7.74 (m, 1H), 7.71–7.54 (m, 2H), 7.35–7.32 (m, 1H), 6.13–6.10 (m, 1H), 3.97–3.80 (m, 6H), 3.46–3.39 (m, 2H), 3.25–3.23 (m, 2H), 1.65–1.46 (m, 1H), 1.45–1.43 (m, 2H), 0.93 (d, J = 6.3 Hz, 6H). MS (ES+) m/z 450.0 (M + H) $^{+}$.

Piperazine-1-yl-(2-trifluoromethylphenyl)methanone (4a). To a stirred solution of *tert*-butyl piperazine-1-carboxylate (6.00 g, 32.2 mmol) and DIPEA (16.8 mL, 96.7 mmol) in DCM (350 mL) at 0 $^{\circ}$ C was added a solution of 2-trifluoromethylbenzoyl chloride (5.3 mL, 36.1 mmol). The resulting mixture was stirred at room temperature for 16 h, and water (80 mL) was added. The organic layer was washed with water (2 \times 150 mL), dried over Na_2SO_4 , filtered, and concentrated in vacuo to provide a yellow oil (11.50 g, 32.1 mmol). This yellow oil was dissolved in 200 mL of 1:4 mixture of trifluoroacetic acid and DCM, and the mixture was stirred at room temperature for 4 h. After removal of the solvents, the residue was dissolved in DCM (500 mL) and washed with 1 N NaOH (100 mL), water (80 mL), and brine (80 mL). The organic layer was dried over anhydrous Na_2SO_4 , filtered, and concentrated to afford the product **4a** as an oil in 95% yield (7.93 g, 95% yield). ^1H NMR (300 MHz, CDCl_3) δ 7.73–7.51 (m, 3H), 7.34–7.32 (m, 1H), 4.83 (br s, 1H), 4.15–4.07 (m, 1H), 3.91–3.78 (m, 1H), 3.48–2.91 (m, 6H). MS (ES+) m/z 259.1 (M + H) $^{+}$.

5-(4-(2-(Trifluoromethyl)benzoyl)piperazin-1-yl)pyrazine-2-carboxylic Acid (4b). A mixture of methyl 5-chloropyrazine-2-

carboxylate (172 mg, 1.0 mmol), piperazine-1-yl-(2-trifluoromethylphenyl)methanone **4a** (387 mg, 1.5 mmol), DBU (0.6 mL, 4.0 mmol), and Bu_4NI (18.8 mg, 0.05 mmol) in DMF (3 mL) was heated at 80 $^{\circ}$ C for 70 h and then diluted with EtOAc (100 mL). The resulting mixture was washed with brine (4 \times 100 mL), dried over anhydrous MgSO_4 , and concentrated. The residue was dissolved in 4 mL of MeOH/water mixture (3:1), and LiOH (48 mg, 2.0 mmol) was added. The reaction mixture was stirred at room temperature overnight and then concentrated. The residue was diluted with water (20 mL), and the pH of the resulting aqueous solution was adjusted to \sim 5 with 5% HCl solution. This solution was then extracted with DCM (3 \times 50 mL). The combined organic layer was washed with brine, dried over anhydrous MgSO_4 , and concentrated. The residue was purified by column chromatography to afford **4b** as a white solid (263 mg, 69% yield). MS (ES+) m/z 381.2 (M + H) $^{+}$.

N-Isopentyl-5-(4-(2-(trifluoromethyl)benzoyl)piperazin-1-yl)pyrazine-2-carboxamide (4). 5-(4-(2-(Trifluoromethyl)benzoyl)piperazin-1-yl)pyrazine-2-carboxylic acid **4b** (38 mg, 0.10 mmol) was dissolved in DCM (3 mL), followed by the addition of HOBt monohydrate (23 mg, 0.15 mmol), EDCI (28.8 mg, 0.19 mmol), DIPEA (0.5 mL, 2.9 mmol), and isoamylamine (17.5 μ L, 0.15 mmol). The mixture was stirred at room temperature for 18 h and diluted with EtOAc (20 mL). The organic layer was washed with 5% HCl solution, brine, dried over anhydrous Na_2SO_4 , and concentrated. The residue was purified by preparative TLC to afford **4** as white solid (3.5 mg, 8% yield). ^1H NMR (300 MHz, CDCl_3) δ 8.84 (s, 1H), 7.95 (s, 1H), 7.73 (d, J = 7.5 Hz, 1H), 7.63–7.55 (m, 2H), 7.46–7.42 (m, 1H), 7.35 (d, J = 7.2 Hz, 1H), 4.02–3.99 (m, 1H), 3.90–3.68 (m, 3H), 3.67–3.63 (m, 2H), 3.49–3.41 (m, 2H), 3.34–3.30 (m, 2H), 1.71–1.47 (m, 3H), 0.95 (d, J = 6.6 Hz, 6H). MS (ES+) m/z 450.1 (M + H) $^{+}$.

5-Bromopyrimidine-2-carbonitrile (5a). To a vial containing sodium cyanide (0.27 g, 5.43 mmol) and DABCO (0.087 g, 0.80 mmol) in 3 mL of water was added DMSO (3 mL) under nitrogen atmosphere, followed by the addition of 5-bromo-2-chloropyrimidine (1.00 g, 5.17 mmol) in DMSO (3 mL). The reaction mixture gradually turned brown over 2 h. The reaction mixture was diluted with ethyl acetate (75 mL), washed with water, 1 N HCl, saturated NaHCO_3 solution, and brine, dried over MgSO_4 , filtered, and concentrated in vacuo to yield the product as a yellow solid (0.86 g, 89% yield). MS (ES+) m/z 183.9 (M + H) $^{+}$.

5-(4-(2-(Trifluoromethyl)benzoyl)piperazin-1-yl)pyrimidine-2-carbonitrile (5b). A mixture of 5-bromopyrimidine-2-carbonitrile (0.86 g, 4.6 mmol) obtained above, CsCO_3 (6.00 g, 18.0 mmol) and piperazine-1-yl-(2-trifluoromethylphenyl)methanone **4a** (1.35 g, 4.6 mmol) in 20 mL of anhydrous NMP was heated to 80 $^{\circ}$ C overnight. After removal of the solvent, the residue was dissolved in ethyl acetate (150 mL), and washed with 1 N HCl solution, water, saturated NaHCO_3 solution, and brine and then dried over anhydrous MgSO_4 . The residue obtained after removal of the solvent was purified by column chromatography. The product **5b** was obtained as a white solid (0.63 g, 38% yield). MS (ES+) m/z 362.2 (M + H) $^{+}$.

N-Hexyl-5-(4-(2-(trifluoromethyl)benzoyl)piperazin-1-yl)pyrimidine-2-carboxamide (5). A mixture of 5-[4-(2-trifluoromethylbenzoyl)piperazin-1-yl]pyrimidine-2-carbonitrile **5b** (0.050 g, 0.14 mmol), hexylamine (0.015 mg, 0.15 mmol), water (5 μ L, 0.28 mmol), and dichloro-tris(triphenylphosphine)ruthenium(II) (4.0 mg, 0.004 mmol) in 1,2-dimethoxyethane (0.2 mL) in a sealed tube was heated to 160 $^{\circ}$ C for three days. The reaction mixture was diluted with dichloromethane and then loaded onto a preparative thin layer chromatography plate developed using ethyl acetate/hexanes = 4:1 to afford the crude compound. The pure compound was obtained as a white solid after recrystallization from isopropyl alcohol (8.9 mg, 14% yield). ^1H NMR (300 MHz, CDCl_3) δ 8.39 (s, 2H), 7.81–7.72 (m, 2H), 7.69–7.52 (m, 2H), 7.39–7.36 (m, 1H), 4.16–3.88 (m, 2H), 3.71–3.21 (m, 8H), 1.65–1.58 (m, 2H), 1.42–1.22 (m, 6H), 0.93 (t, J = 6.9 Hz, 3H). MS (ES+) m/z 464 (M + H) $^{+}$.

5-Hydroxy-N-isopentylpicolinamide (6a). To a solution of 5-hydroxypicolinic acid (103 mg, 0.74 mmol) in DCM (6 mL) was added DIPEA (0.13 mL, 1.48 mmol), HOBt monohydrate (100 mg,

0.74 mmol), and EDCI (142 mg, 0.74 mmol). The resulting mixture was stirred at room temperature for 15 min, followed by the addition of isoamylamine (68 μ L, 0.74 mmol). The reaction mixture was stirred at room temperature for 23 h, and DCM (50 mL) was added. The organic layer was washed with diluted HCl solution, brine, dried over anhydrous Na_2SO_4 , and concentrated. The residue was purified by column chromatography to afford **6a** as a colorless gum (0.86 g, 56% yield). MS (ES+) m/z 209.1 ($M + H$)⁺.

6-(Isopentylcarbamoyl)pyridin-3-yl trifluoromethanesulfonate (6b). To a solution of 5-hydroxy-*N*-isopentylpicolinamide **6a** (82 mg, 0.39 mmol) in pyridine (2 mL) was added TiF_4 (74 μ L, 0.4 mmol) at 0 °C. The resulting mixture was stirred at 0 °C for 10 min and then at room temperature for 25 h, followed by the addition of water (50 mL). The mixture was extracted with ether (3 \times 40 mL). The combined organic layer was washed with water, brine, dried over anhydrous MgSO_4 , and concentrated. The residue was purified by column chromatography to afford **6b** as colorless oil (50 mg, 38% yield). MS (ES+) m/z 341.2 ($M + H$)⁺.

tert-Butyl 4-(6-(isopentylcarbamoyl)pyridin-3-yl)piperazine-1-carboxylate (6c). A 50 mL flask was charged with Cs_2CO_3 (67 mg, 0.21 mmol), $\text{Pd}(\text{OAc})_2$ (1.7 mg, 0.0074 mmol), and BINAP (6.9 mg, 0.011 mmol) and flashed with argon for 30 min. A solution of 6-(isopentylcarbamoyl)pyridin-3-yl trifluoromethanesulfonate **6b** (50 mg, 0.15 mmol) and *tert*-butyl piperazine-1-carboxylate (33 mg, 0.18 mmol) in toluene (2 mL) was added via a syringe. The reaction mixture was heated at 98 °C for 19 h and then cooled to room temperature. Toluene (20 mL) was added, and the mixture was filtered. The filtrate was concentrated in vacuo, and the residue was purified by column chromatography to provide **6c** as a white solid (9 mg, 14% yield).

***N*-Isopentyl-5-(4-(2-(trifluoromethyl)benzoyl)piperazin-1-yl)picolinamide (6).** This compound was synthesized analogously to compound **3** and was isolated as a white solid (10.4 mg, 97% yield). ¹H NMR (300 MHz, CDCl_3) δ 8.15–8.14 (m, 1H), 8.06 (s, 1H), 7.76–7.72 (m, 1H), 7.63–7.58 (m, 2H), 7.37–7.34 (m, 1H), 7.24–7.19 (m, 2H), 4.10–3.95 (m, 4H), 3.49–3.36 (m, 4H), 3.23–3.19 (m, 2H), 1.73–1.66 (m, 2H), 1.55–1.53 (m, 1H), 0.96 (d, J = 6.5 Hz, 6H). MS (ES+) m/z 449.0 ($M + H$)⁺.

Methyl 6-(4-(2-(trifluoromethyl)benzoyl)piperazin-1-yl)pyridazine-3-carboxylate (7a). To a solution of 6-chloropyridazine-3-carboxylic acid methyl ester (4.36 g, 25.3 mmol) in 1,4-dioxane (100 mL) was added 1-(2-(trifluoromethyl)benzoyl)piperazine hydrochloride (7.80 g, 26.5 mmol), K_2CO_3 (10.14 g, 73.4 mmol), and Bu_4NI (0.071 g, 0.19 mmol). The reaction mixture was heated to reflux for 24 h and then concentrated. The residue was washed with water and ether to afford **7a** as a white solid (8.67 g, 87% yield). ¹H NMR (300 MHz, CDCl_3) δ 7.92 (d, J = 9.3 Hz, 1H), 7.77 (d, J = 7.5 Hz, 1H), 7.64–7.51 (m, 2H), 7.34 (d, J = 7.5 Hz, 1H), 6.89 (d, J = 9.3 Hz, 1H), 4.11–3.35 (m, 6H), 3.33 (t, J = 5.1 Hz, 2H). MS (ES+) m/z 395.1 ($M + H$)⁺.

6-(4-(2-(trifluoromethyl)benzoyl)piperazin-1-yl)pyridazine-3-carboxylic Acid (7b). To a solution of 6-[4-(2-(trifluoromethyl)benzoyl)piperazin-1-yl]pyridazine-3-carboxylic acid methyl ester (8.38 g, 21.2 mmol) in THF (100 mL) and water (50 mL) was added lithium hydroxide monohydrate (1.80 g, 42.9 mmol). The reaction mixture was stirred at room temperature for 6 h, and the pH of the mixture was adjusted to ~5 with 5% hydrochloric acid at 0 °C. THF was removed in vacuo. Ethyl acetate (100 mL) was added to the residue and a white solid precipitated. The solid was isolated by filtration and washed with ether and dried to afford **7b** as a white solid (15.4 g, 98% yield). ¹H NMR (300 MHz, CDCl_3) δ 8.02 (d, J = 9.3 Hz, 1H), 7.75–7.72 (m, 1H), 7.66–7.5 (m, 2H), 7.37–7.35 (m, 1H), 7.01 (d, J = 9.3 Hz, 1H), 4.13–4.03 (m, 1H), 3.95–3.64 (m, 5H), 3.38–3.34 (m, 2H). MS (ES+) m/z 381.1 ($M + H$)⁺.

***N*-(Pyridin-2-yl)-6-(4-(2-(trifluoromethyl)benzoyl)piperazin-1-yl)pyridazine-3-carboxamide (26).** To a solution of 6-[4-(2-(trifluoromethyl)benzoyl)piperazin-1-yl]pyridazine-3-carboxylic acid (0.10 g, 0.26 mmol) in chloroform (10 mL) was added thionyl chloride (0.5 mL) and a drop of DMF. The reaction mixture was refluxed for 18 h, and the volatiles were removed in vacuo. The residue

was dissolved in dichloromethane (2 mL). This solution was added dropwise at room temperature to a solution of 2-aminopyridine (38 mg, 0.40 mmol) and triethylamine (0.1 mL) in dichloromethane (2 mL). The reaction mixture was stirred at room temperature for 4 h and diluted with EtOAc (100 mL) and washed with water (3 \times 10 mL) and brine (2 \times 10 mL). The organic layer was dried over Na_2SO_4 and evaporated to provide a crude product, which was purified by column chromatography (hexane/EtOAc = 1:1 to pure EtOAc) to afford **26** as a white solid (44 mg, 37% yield). ¹H NMR (300 MHz, CDCl_3) δ 10.30 (s, 1H), 8.35 (m, 2H), 8.09 (d, J = 9.3 Hz, 1H), 7.75–6.69 (m, 2H), 7.65–7.52 (m, 2H), 7.35 (d, J = 7.2 Hz, 1H), 7.09–6.96 (m, 2H), 4.10–4.02 (m, 1H), 3.92–3.71 (m, 5H), 3.37–3.34 (m, 2H). MS (ES+) m/z 457.3 ($M + H$)⁺.

The general procedure described for **26** was followed for the preparation of compounds **7** and **9–35**, using the appropriate amines for amide formation.

***N*-Isopentyl-6-(4-(2-(trifluoromethyl)benzoyl)piperazin-1-yl)pyridazine-3-carboxamide (7).** White solid (73% yield). ¹H NMR (500 MHz, CDCl_3) δ 8.05 (d, J = 9.6 Hz, 1H), 7.98 (t, J = 6.4 Hz, 1H), 7.77–7.73 (m, 1H), 7.66–7.62 (m, 1H), 7.59–7.55 (m, 1H), 7.39–7.35 (m, 1H), 7.00 (d, J = 9.6 Hz, 1H), 4.08–4.04 (m, 1H), 3.90–3.87 (m, 2H), 3.82–3.64 (m, 3H), 3.51–3.47 (m, 2H), 3.38–3.34 (m, 2H), 1.72–1.68 (m, 1H), 1.52–1.49 (m, 2H), 0.95 (d, J = 7.1 Hz, 6H). MS (ES+) m/z 450.3 ($M + H$)⁺.

***N*-(Cyclopropylmethyl)-6-(4-(2-(trifluoromethyl)benzoyl)piperazin-1-yl)pyridazine-3-carboxamide (9).** White solid (31% yield). ¹H NMR (500 MHz, CDCl_3) δ 8.16–7.88 (m, 2H), 7.75 (d, J = 7.8 Hz, 1H), 7.68–7.46 (m, 2H), 7.18 (d, J = 7.8 Hz, 1H), 7.00 (d, J = 9.3 Hz, 1H), 4.17–3.64 (m, 6H), 3.21–3.12 (m, 4H), 1.07–1.00 (m, 1H), 0.61–0.44 (m, 2H), 0.26–0.20 (m, 2H). MS (ES+) m/z 434.4 ($M + H$)⁺.

***N*-(3-Cyclopropylpropyl)-6-(4-(2-(trifluoromethyl)benzoyl)piperazin-1-yl)pyridazine-3-carboxamide (10).** White solid (28% yield). ¹H NMR (400 MHz, CDCl_3) δ 8.04 (d, J = 9.3 Hz, 1H), 7.89 (t, J = 5.8 Hz, 1H), 7.73 (t, J = 7.4 Hz, 1H), 7.65 (t, J = 7.3 Hz, 1H), 7.58 (t, J = 7.6 Hz, 1H), 7.38 (d, J = 7.2 Hz, 1H), 6.99 (d, J = 9.3 Hz, 1H), 4.08–3.67 (m, 6H), 3.54–3.46 (m, 2H), 3.39–3.31 (m, 2H), 1.77–1.66 (m, 2H), 1.34–1.23 (m, 2H), 0.72–0.62 (m, 1H), 0.45–0.36 (m, 2H), 0.06–0.04 (m, 2H). MS (ES+) m/z 462.2 ($M + H$)⁺.

***N*-(4-Cyclopropylbutyl)-6-(4-(2-(trifluoromethyl)benzoyl)piperazin-1-yl)pyridazine-3-carboxamide (11).** White solid (21% yield). ¹H NMR (300 MHz, CDCl_3) δ 8.03 (d, J = 9.4 Hz, 1H), 7.88–7.84 (m, 1H), 7.72 (d, J = 7.5 Hz, 1H), 7.60–7.56 (m, 2H), 7.34 (d, J = 7.5 Hz, 1H), 6.98 (d, J = 9.4 Hz, 1H), 4.05–4.02 (m, 1H), 3.89–3.62 (m, 5H), 3.48–3.31 (m, 4H), 1.64–1.41 (m, 4H), 1.21–1.19 (m, 2H), 0.61–0.59 (m, 1H), 0.39–0.30 (m, 2H), –0.06–0.02 (m, 2H). MS (ES+) m/z 476.1 ($M + H$)⁺.

***N*-(3-Hydroxy-3-methylbutyl)-6-(4-(2-(trifluoromethyl)benzoyl)piperazin-1-yl)pyridazine-3-carboxamide (12).** White solid (46% yield). ¹H NMR (500 MHz, CDCl_3) δ 8.30 (br s, 1H), 8.05 (d, J = 9.8 Hz, 1H), 7.78–7.74 (m, 1H), 7.68–7.62 (m, 1H), 7.60–7.55 (m, 1H), 7.40–7.35 (m, 1H), 6.98 (d, J = 9.8 Hz, 1H), 4.07–4.04 (m, 1H), 3.91–3.85 (m, 2H), 3.81–3.69 (m, 3H), 3.67–3.60 (m, 2H), 3.40–3.32 (m, 3H), 1.80 (t, J = 7.5 Hz, 2H), 1.30 (s, 6H). MS (ES+) m/z 466.0 ($M + H$)⁺.

***N*-(2-Ethoxyethyl)-6-(4-(2-(trifluoromethyl)benzoyl)piperazin-1-yl)pyridazine-3-carboxamide (13).** White solid (25% yield). ¹H NMR (500 MHz, CDCl_3) δ 8.18 (t, J = 5.6 Hz, 1H), 8.07 (d, J = 9.6 Hz, 1H), 7.78–7.74 (m, 1H), 7.67–7.63 (m, 1H), 7.61–7.57 (m, 1H), 7.40–7.36 (m, 1H), 7.00 (d, J = 9.6 Hz, 1H), 4.09–4.03 (m, 1H), 3.93–3.89 (m, 2H), 3.83–3.65 (m, 5H), 3.62–3.58 (m, 2H), 3.54–3.50 (q, 2H), 3.38–3.33 (m, 2H), 1.20 (t, J = 8.1 Hz, 3H). MS (ES+) m/z 452.0 ($M + H$)⁺.

***N*-Pentyl-6-(4-(2-(trifluoromethyl)benzoyl)piperazin-1-yl)pyridazine-3-carboxamide (14).** White solid (94% yield); mp 123–125 °C. ¹H NMR (300 MHz, CDCl_3) δ 8.04 (d, J = 9.6 Hz, 1H), 7.86–7.82 (m, 1H), 7.80–7.70 (m, 1H), 7.68–7.52 (m, 2H), 7.40–7.32 (m, 1H), 6.99 (d, J = 9.6 Hz, 1H), 4.06–4.00 (m, 1H), 3.91–3.69 (m, 5H), 3.50–3.30 (m, 4H), 1.62–1.55 (m, 2H), 1.37–1.31 (m, 4H), 0.84 (t, J = 6.9 Hz, 3H). MS (ES+) m/z 450.2 ($M + H$)⁺.

N-Hexyl-6-(4-(2-(trifluoromethyl)benzoyl)piperazin-1-yl)pyridazine-3-carboxamide (15). White solid (35% yield). ¹H NMR (300 MHz, CDCl₃) δ 8.02 (d, *J* = 9.6 Hz, 1H), 7.85 (t, *J* = 5.7 Hz, 1H), 7.74–7.70 (m, 1H), 7.57–7.54 (m, 2H), 7.36–7.32 (m, 1H), 6.97 (d, *J* = 9.6 Hz, 1H), 4.02–3.96 (m, 1H), 3.90–3.64 (m, 5H), 3.48–3.28 (m, 4H), 1.61–1.56 (m, 2H), 1.31–1.27 (m, 6H), 0.85 (t, *J* = 6.9 Hz, 3H). MS (ES+) *m/z* 464.0 (M + H)⁺.

N-Heptyl-6-(4-(2-(trifluoromethyl)benzoyl)piperazin-1-yl)pyridazine-3-carboxamide (16). White solid (41% yield). ¹H NMR (300 MHz, CDCl₃) δ 8.05 (d, *J* = 9.9 Hz, 1H), 7.85 (t, *J* = 5.7 Hz, 1H), 7.74–7.70 (m, 1H), 7.60–7.57 (m, 2H), 7.36–7.33 (m, 1H), 7.00–6.96 (m, 1H), 4.05–4.00 (m, 1H), 3.94–3.64 (m, 5H), 3.47–3.28 (m, 4H), 1.61–1.57 (m, 2H), 1.32–1.25 (m, 8H), 0.84 (t, *J* = 6.3 Hz, 3H). MS (ES+) *m/z* 478.2 (M + H)⁺.

N-(4-Chlorophenyl)-6-(4-(2-(trifluoromethyl)benzoyl)piperazin-1-yl)pyridazine-3-carboxamide (17). White solid (67% yield). ¹H NMR (300 MHz, CDCl₃) δ 9.79 (s, 1H), 8.08 (d, *J* = 9.6 Hz, 1H), 7.82–7.55 (m, 5H), 7.36–7.28 (m, 3H), 7.02 (d, *J* = 9.6 Hz, 1H), 4.10–4.00 (m, 1H), 3.93–3.68 (m, 5H), 3.35 (t, *J* = 5.1 Hz, 2H). MS (ES+) *m/z* 490.1 (M + H)⁺.

N-Phenyl-6-(4-(2-(trifluoromethyl)benzoyl)piperazin-1-yl)pyridazine-3-carboxamide (18). White solid (99% yield). ¹H NMR (300 MHz, CDCl₃) δ 8.18 (t, *J* = 5.4 Hz, 1H), 8.07 (dd, *J* = 9.6, 0.9 Hz, 1H), 7.73 (d, *J* = 7.6 Hz, 1H), 7.65–7.50 (m, 2H), 7.37–7.25 (m, 6H), 6.99 (d, *J* = 9.6 Hz, 1H), 4.08–4.00 (m, 1H), 3.90–3.64 (m, 5H), 3.33 (t, *J* = 5.4 Hz, 2H). MS (ES+) *m/z* 456.3 (M + H)⁺.

N-Benzyl-6-(4-(2-(trifluoromethyl)benzoyl)piperazin-1-yl)pyridazine-3-carboxamide (19). White solid (98% yield). MS (ES+) *m/z* 470.6 (M + H)⁺.

N-Phenethyl-6-(4-(2-(trifluoromethyl)benzoyl)piperazin-1-yl)pyridazine-3-carboxamide (20). White solid (82% yield). ¹H NMR (300 MHz, CDCl₃) δ 8.03 (d, *J* = 9.6 Hz, 1H), 7.94–7.90 (m, 1H), 7.75–7.72 (m, 1H), 7.65–7.57 (m, 2H), 7.36–7.09 (m, 6H), 6.97 (d, *J* = 9.6 Hz, 1H), 4.11–4.00 (m, 1H), 3.90–3.65 (m, 7H), 3.36–3.30 (m, 2H), 2.91 (t, *J* = 7.2 Hz, 2H). MS (ES+) *m/z* 484 (M + H)⁺.

N-(3-Phenylpropyl)-6-(4-(2-(trifluoromethyl)benzoyl)piperazin-1-yl)pyridazine-3-carboxamide (21). White solid (15% yield). ¹H NMR (500 MHz, CDCl₃) δ 8.05 (d, *J* = 9.3 Hz, 1H), 7.93 (t, *J* = 6.3 Hz, 1H), 7.74 (d, *J* = 7.6 Hz, 1H), 7.63 (t, *J* = 7.4 Hz, 1H), 7.56 (t, *J* = 7.4 Hz, 1H), 7.39 (d, *J* = 7.6 Hz, 1H), 7.29–7.13 (m, 5H), 6.92 (d, *J* = 9.3 Hz, 1H), 4.12–3.29 (m, 10H), 2.68 (t, *J* = 5.7 Hz, 2H), 2.02–1.83 (m, 2H).

N-(2-Phenylpropyl)-6-(4-(2-(trifluoromethyl)benzoyl)piperazin-1-yl)pyridazine-3-carboxamide (22). White solid (63% yield). ¹H NMR (500 MHz, CDCl₃) δ 7.97 (d, *J* = 9.5 Hz, 1H), 7.82–7.78 (m, 1H), 7.70–7.67 (m, 1H), 7.59–7.55 (m, 1H), 7.52–7.49 (m, 1H), 7.32–7.28 (m, 1H), 7.25–7.22 (m, 2H), 7.20–7.12 (m, 3H), 6.92 (d, *J* = 9.5 Hz, 1H), 3.98 (m, 1H), 3.80 (m, 2H), 3.74–3.60 (m, 4H), 3.53 (m, 1H), 3.28 (br s, 2H), 3.02–2.98 (m, 1H), 1.28 (d, *J* = 6.7 Hz, 3H). MS (ES+) *m/z* 474.4 (M + H)⁺.

(R)-N-(2-Hydroxy-2-phenylethyl)-6-(4-(2-(trifluoromethyl)benzoyl)piperazin-1-yl)pyridazine-3-carboxamide (23). White solid (65% yield). ¹H NMR (500 MHz, CDCl₃) δ 8.26 (t, *J* = 9.3 Hz, 1H), 8.01 (d, *J* = 9.6 Hz, 1H), 7.73 (d, *J* = 7.5 Hz, 1H), 7.65–7.53 (m, 2H), 7.46–7.21 (m, 6H), 6.96 (d, *J* = 9.6 Hz, 1H), 4.94–4.90 (m, 1H), 4.05–3.98 (m, 1H), 3.90–3.52 (m, 7H), 3.30 (t, *J* = 5.1 Hz, 2H). MS (ES+) *m/z* 500.0 (M + H)⁺.

(S)-N-(2-Hydroxy-2-phenylethyl)-6-(4-(2-(trifluoromethyl)benzoyl)piperazin-1-yl)pyridazine-3-carboxamide (24). White solid (64% yield). ¹H NMR (500 MHz, CDCl₃) δ 8.27 (t, *J* = 9.3 Hz, 1H), 8.01 (d, *J* = 9.6 Hz, 1H), 7.73 (d, *J* = 7.5 Hz, 1H), 7.65–7.53 (m, 2H), 7.41–7.23 (m, 6H), 6.98 (d, *J* = 9.3 Hz, 1H), 4.95–4.91 (m, 1H), 4.13–4.00 (m, 1H), 3.90–3.53 (m, 7H), 3.32 (t, *J* = 5.1 Hz, 2H). MS (ES+) *m/z* 522.0 (M + Na)⁺.

N-(Pyridin-2-ylmethyl)-6-(4-(2-(trifluoromethyl)benzoyl)piperazin-1-yl)pyridazine-3-carboxamide (27). White solid (48% yield); mp 179–181 °C. ¹H NMR (300 MHz, CDCl₃) δ 8.81 (t, *J* = 5.1 Hz, 1H), 8.59 (d, *J* = 4.8 Hz, 1H), 8.12 (d, *J* = 7.2 Hz, 1H), 7.78–7.50 (m, 4H), 7.37 (t, *J* = 8.4 Hz, 1H), 7.21–7.13 (m, 1H), 6.93 (d, *J* =

7.2 Hz, 1H), 4.83 (d, *J* = 5.4 Hz, 2H), 4.17–3.66 (m, 6H), 3.37 (t, *J* = 5.1 Hz, 2H). MS (ES+) *m/z* 471.0 (M + H)⁺.

N-(1H-Benzo[d]imidazol-2-yl)-6-(4-(2-(trifluoromethyl)benzoyl)piperazin-1-yl)pyridazine-3-carboxamide (28). White solid (31% yield); mp 231–232 °C. ¹H NMR (300 MHz, CDCl₃) δ 8.07 (d, *J* = 9.6 Hz, 1H), 7.73 (d, *J* = 8.1 Hz, 1H), 7.66–7.49 (m, 4H), 7.35 (d, *J* = 7.5 Hz, 1H), 7.24–7.19 (m, 2H), 6.97 (d, *J* = 9.6 Hz, 1H), 4.15–4.03 (m, 1H), 3.91–3.71 (m, 5H), 3.34 (t, *J* = 4.8 Hz, 2H). MS (ES+) *m/z* 496.5 (M + H)⁺.

N-((5-Methylpyrazin-2-yl)methyl)-6-(4-(2-(trifluoromethyl)benzoyl)piperazin-1-yl)pyridazine-3-carboxamide (29). White solid (71% yield); mp 149–151 °C (ethyl acetate/hexanes). ¹H NMR (300 MHz, CDCl₃) δ 8.67–8.62 (m, 1H), 8.46 (s, 1H), 8.34 (s, 1H), 8.00 (d, *J* = 9.3 Hz, 1H), 7.69 (d, *J* = 7.8 Hz, 1H), 7.61–7.49 (m, 2H), 7.31 (d, *J* = 7.8 Hz, 1H), 6.95 (d, *J* = 9.3 Hz, 1H), 4.74 (d, *J* = 5.7 Hz, 2H), 4.07–3.62 (m, 6H), 3.30 (t, *J* = 5.1 Hz, 2H), 2.49 (s, 3H). MS (ES+) *m/z* 486.4 (M + H)⁺.

N-(Thiazol-2-ylmethyl)-6-(4-(2-(trifluoromethyl)benzoyl)piperazin-1-yl)pyridazine-3-carboxamide (30). White solid (62% yield); mp 153–154 °C (ethyl acetate/hexanes). ¹H NMR (300 MHz, CDCl₃) δ 8.55 (t, *J* = 6.0 Hz, 1H), 8.02 (d, *J* = 9.3 Hz, 1H), 7.75–7.50 (m, 4H), 7.25–7.23 (m, 1H), 6.94 (d, *J* = 9.3 Hz, 1H), 4.96 (d, *J* = 6.0 Hz, 2H), 4.11–3.69 (m, 6H), 3.32 (t, *J* = 5.1 Hz, 2H). MS (ES+) *m/z* 477.4 (M + H)⁺.

N-(Oxazol-4-ylmethyl)-6-(4-(2-(trifluoromethyl)benzoyl)piperazin-1-yl)pyridazine-3-carboxamide (31). White solid (20% yield); mp 76–78 °C (EtOAc/hexanes). ¹H NMR (300 MHz, CDCl₃) δ 8.25 (t, *J* = 5.7 Hz, 1H), 8.01 (d, *J* = 9.3 Hz, 1H), 7.82 (s, 1H), 7.72 (d, *J* = 7.8 Hz, 1H), 7.64–7.51 (m, 3H), 7.34 (d, *J* = 7.8 Hz, 1H), 6.97 (d, *J* = 9.3 Hz, 1H), 4.58 (d, *J* = 5.7 Hz, 2H), 4.12–3.64 (m, 6H), 3.34–3.30 (m, 2H). MS (ES+) *m/z* 461.2 (M + H)⁺.

N-(Oxazol-2-ylmethyl)-6-(4-(2-(trifluoromethyl)benzoyl)piperazin-1-yl)pyridazine-3-carboxamide (32). White solid (22% yield); mp 94–97 °C. ¹H NMR (300 MHz, CDCl₃) δ 8.40 (d, *J* = 5.7 Hz, 1H), 8.01 (d, *J* = 9.3 Hz, 1H), 7.70 (d, *J* = 7.8 Hz, 1H), 7.62–7.44 (m, 3H), 7.33 (d, *J* = 7.8 Hz, 1H), 7.03–6.89 (m, 2H), 4.77 (d, *J* = 5.7 Hz, 2H), 4.11–3.66 (m, 6H), 3.37–3.30 (m, 2H). MS (ES+) *m/z* 461.2 (M + H)⁺.

N-((5-Methylfuran-2-yl)methyl)-6-(4-(2-(trifluoromethyl)benzoyl)piperazin-1-yl)pyridazine-3-carboxamide (33). White solid (87% yield). ¹H NMR (300 MHz, CDCl₃) δ 8.02 (t, *J* = 5.7 Hz, 1H), 7.98 (d, *J* = 9.6 Hz, 1H), 7.71–7.49 (m, 3H), 7.32 (d, *J* = 7.2 Hz, 1H), 6.96 (d, *J* = 9.6 Hz, 1H), 6.16 (d, *J* = 2.7 Hz, 1H), 5.83 (d, *J* = 2.7 Hz, 1H), 4.54 (d, *J* = 2.7 Hz, 1H), 4.03–3.62 (m, 6H), 3.32–3.26 (m, 2H), 2.20 (s, 3H). MS (ES+) *m/z* 474.4 (M + H)⁺.

6-(4-(2-(Trifluoromethyl)benzoyl)piperazin-1-yl)-N-((5-(trifluoromethyl)furan-2-yl)methyl)-pyridazine-3-carboxamide (34). White solid (77% yield); mp 151–152 °C (EtOAc/hexanes). ¹H NMR (300 MHz, CDCl₃) δ 8.22 (t, *J* = 6.0 Hz, 1H), 8.01 (d, *J* = 9.3 Hz, 1H), 7.72 (d, *J* = 7.8 Hz, 1H), 7.64–7.51 (m, 2H), 7.34 (d, *J* = 7.8 Hz, 1H), 6.98 (d, *J* = 9.3 Hz, 1H), 6.69–6.68 (m, 1H), 6.34–6.33 (m, 1H), 4.66 (d, *J* = 6.0 Hz, 2H), 4.14–3.66 (m, 6H), 3.33 (t, *J* = 5.4 Hz, 2H). MS (ES+) *m/z* 528.2 (M + H)⁺.

N-((1H-Pyrazol-3-yl)methyl)-6-(4-(2-(trifluoromethyl)benzoyl)piperazin-1-yl)pyridazine-3-carboxamide (35). White solid (37% yield); mp 102–103 °C (EtOAc/hexanes). ¹H NMR (300 MHz, CDCl₃) δ 8.43 (t, *J* = 6.0 Hz, 1H), 8.03 (d, *J* = 9.6 Hz, 1H), 7.72 (d, *J* = 7.8 Hz, 1H), 7.61–7.49 (m, 3H), 7.34 (d, *J* = 7.8 Hz, 1H), 6.97 (d, *J* = 9.6 Hz, 1H), 6.25 (d, *J* = 1.8 Hz, 1H), 5.39 (br s, 1H), 4.68 (d, *J* = 6.0 Hz, 2H), 4.06–3.65 (m, 6H), 3.39–3.33 (m, 2H). MS (ES+) *m/z* 460.2 (M + H)⁺.

N-(2-Oxo-2-phenylethyl)-6-(4-(2-(trifluoromethyl)benzoyl)piperazin-1-yl)pyridazine-3-carboxamide (25). To a solution of (R)-N-(2-hydroxy-2-phenylethyl)-6-(4-(2-(trifluoromethyl)benzoyl)piperazin-1-yl)pyridazine-3-carboxamide **23** (0.52 g, 1.03 mmol) in DCM (10 mL) was added Dess–Martin periodinate (0.53 g) in one portion under stirring in a cold water bath. After stirring in a cold water bath for 15 min, the reaction mixture was warmed to room temperature and stirred for 2 h and then was diluted with diethyl ether (20 mL). The mixture was poured into a solution of sodium thiosulfate (1.18 g, 7.44 mmol) in saturated aqueous sodium

biocarbonate (29 mL). The mixture was extracted with EtOAc (100 mL). The organic layer was washed with saturated aqueous NaHCO₃ (2 × 15 mL) and water (2 × 15 mL). The combined aqueous washes were then extracted with EtOAc (2 × 80 mL). The combined organic phases were dried over anhydrous Na₂SO₄ and filtered. The filtrate was concentrated in vacuo. The residue was purified by column chromatography eluted with hexane/EtOAc (1:1), hexane/EtOAc (1:2), and EtOAc (100%). The product was obtained as a white powder (0.26 g, 51% yield); mp 196–198 °C. ¹H NMR (300 MHz, CDCl₃) δ 8.75–8.70 (m, 1H), 8.06–7.97 (m, 3H), 7.74 (d, *J* = 7.5 Hz, 1H), 7.66–7.47 (m, 5H), 7.36 (d, *J* = 7.5 Hz, 1H), 6.99 (d, *J* = 9.6 Hz, 1H), 4.96 (d, *J* = 4.8 Hz, 2H), 4.11–4.02 (m, 1H), 3.92–3.70 (m, 5H), 3.42–3.27 (m, 2H). MS (ES+) *m/z* 498.3 (M + H)⁺.

6-Chloro-*N*-(2-cyclopropylethyl)pyridazine-3-carboxamide (8a). To a suspension of 6-chloropyridazine-3-carboxylic acid (3.70 g, 23.0 mmol) in chloroform (30 mL) was added thionyl chloride (5 mL), followed by the addition of a drop of DMF. The resulting reaction mixture was heated to reflux for 11 h, and the volatiles were removed in vacuo. The residue was dissolved in dichloromethane (100 mL), and the resulting solution was cooled to 0 °C, followed by the addition of Et₃N (5.5 mL, 39.0 mmol) and 2-cyclopropylethylamine³⁷ (2.50 g, 29.3 mmol). The reaction mixture was stirred at room temperature for 30 min, diluted with ethyl acetate, washed with water, saturated NaHCO₃, and brine, dried over anhydrous Na₂SO₄, and filtered. The filtrate was concentrated, and the residue was recrystallized from ethyl acetate and hexane to afford **8a** as a white solid in 84% yield (4.40 g). ¹H NMR (300 MHz, CDCl₃) δ 8.26 (d, *J* = 9.0 Hz, 1H), 8.14 (br s, 1H), 3.64–3.53 (m, 2H), 1.62–1.50 (m, 2H), 0.80–0.67 (m, 1H), 0.56–0.51 (m, 2H), 0.18–0.02 (m, 2H).

***N*-(2-cyclopropylethyl)-6-(piperazin-1-yl)pyridazine-3-carboxamide (8b).** A solution of 6-chloro-*N*-(2-cyclopropylethyl)pyridazine-3-carboxamide (7.80 g, 34.0 mmol) and piperazine (8.93 g, 103 mmol) in acetonitrile (100 mL) was heated to reflux for 2 h. The solvent was removed in vacuo, and the residue was dissolved in water (100 mL) and then extracted with dichloromethane (5 × 100 mL). The combined extracts were dried over anhydrous Na₂SO₄ and filtered. The filtrate was concentrated to provide **8b** as a white solid (8.2 g, 88% yield). ¹H NMR (300 MHz, CDCl₃) δ 7.90–7.87 (m, 2H), 6.89 (d, *J* = 9.2 Hz, 1H), 3.78–3.50 (m, 6H), 3.12–2.90 (m, 4H), 1.77–1.49 (m, 2H), 0.83–0.60 (m, 1H), 0.51–0.36 (m, 2H), 0.15–0.01 (m, 2H).

***N*-(2-Cyclopropylethyl)-6-(4-(2-(trifluoromethyl)benzoyl)piperazin-1-yl)pyridazine-3-carboxamide (8).** 2-Trifluoromethylbenzoic chloride (0.33 mL, 2.23 mmol) was added to a solution of *N*-(2-cyclopropylethyl)-6-(piperazin-1-yl)pyridazine-3-carboxamide (0.55 g, 2.00 mmol) and Et₃N (0.4 mL, 2.87 mmol) in dichloromethane (10 mL) at 0 °C. The resulting mixture was stirred for 5 min, and the cooling bath was removed. The stirring was continued for 1 h at room temperature. The reaction mixture was diluted with ethyl acetate (100 mL), washed with water, saturated NaHCO₃, and brine, dried over anhydrous Na₂SO₄, and evaporated. The residue was purified by flash chromatography eluted with ethyl acetate to afford **8** as a white solid (0.83 mg, 92% yield); mp 125–127 °C. ¹H NMR (300 MHz, CDCl₃) δ 8.05 (d, *J* = 9.3 Hz, 1H), 7.96 (t, *J* = 5.7 Hz, 1H), 7.74 (d, *J* = 7.8 Hz, 1H), 7.65–7.52 (m, 2H), 7.35 (d, *J* = 7.8 Hz, 1H), 6.99 (d, *J* = 9.3 Hz, 1H), 4.08–4.00 (m, 1H), 3.97–3.65 (m, 5H), 3.62–3.57 (m, 2H), 3.38–3.22 (m, 2H), 1.55–1.46 (m, 2H), 0.80–0.67 (m, 1H), 0.48–0.42 (m, 2H), 0.10–0.07 (m, 2H). MS (ES+) *m/z* 448.2 (M + H)⁺.

The general procedure described for **8** was followed for the preparation of the following compounds, using the appropriate acid chlorides or acid bromide for the coupling.

***N*-(2-Cyclopropylethyl)-6-(4-(3,3,3-trifluoro-2-methyl-2-(trifluoromethyl)propanoyl)piperazin-1-yl)pyridazine-3-carboxamide (36).** White solid (35% yield). ¹H NMR (300 MHz, CDCl₃) δ 8.02 (d, *J* = 9.5 Hz, 1H), 7.96 (br s, 1H), 6.80 (d, *J* = 9.5 Hz, 1H), 3.91–3.75 (m, 8H), 3.60–3.57 (m, 2H), 1.58–1.48 (m, 5H), 0.78–0.63 (m, 1H), 0.48–0.43 (m, 2H), 0.11–0.04 (m, 2H). MS (ES+) *m/z* 468.2 (M + H)⁺.

6-(4-(2-Chloro-4-(trifluoromethyl)pyrimidine-5-carbonyl)piperazin-1-yl)-*N*-(2-cyclopropylethyl)pyridazine-3-carboxa-

mid (41). White solid (35% yield). ¹H NMR (300 MHz, CDCl₃) δ 8.77 (s, 1H), 8.08 (d, *J* = 9.6 Hz, 1H), 7.97 (t, *J* = 6.3 Hz, 1H), 7.01 (d, *J* = 9.6 Hz, 1H), 4.06–3.68 (m, 6H), 3.55 (q, *J* = 6.9 Hz, 2H), 3.39 (t, *J* = 5.4 Hz, 2H), 1.50 (q, *J* = 6.9 Hz, 2H), 0.76–0.71 (m, 1H), 0.48–0.42 (m, 2H), 0.1–0.05 (m, 2H).

6-(4-(2-Cyanobenzoyl)piperazin-1-yl)-*N*-(2-cyclopropylethyl)pyridazine-3-carboxamide (43). White solid (26% yield). ¹H NMR (300 MHz, CDCl₃) δ 8.05 (d, *J* = 9.6 Hz, 1H), 7.97 (t, *J* = 5.7 Hz, 1H), 7.76–7.72 (m, 1H), 7.69–7.66 (m, 1H), 7.58–7.55 (m, 1H), 7.53–7.43 (m, 1H), 6.99 (d, *J* = 9.6 Hz, 1H), 4.03–3.94 (m, 2H), 3.88–3.85 (m, 4H), 3.58–3.51 (m, 4H), 1.52–1.47 (m, 2H), 0.78–0.65 (m, 1H), 0.48–0.37 (m, 2H), 0.16–0.02 (m, 2H). MS (ES+) *m/z* 405.2 (M + H)⁺.

***N*-(2-Cyclopropylethyl)-6-(4-(2-fluorobenzoyl)piperazin-1-yl)pyridazine-3-carboxamide (45).** White solid (20% yield). ¹H NMR (300 MHz, CDCl₃) δ 8.04 (d, *J* = 9.6 Hz, 1H), 7.98 (t, *J* = 5.7 Hz, 1H), 7.47–7.4 (m, 2H), 7.26–7.21 (m, 1H), 7.15–7.09 (m, 1H), 6.99 (d, *J* = 9.6 Hz, 1H), 3.95–3.78 (m, 6H), 3.58–3.50 (m, 4H), 1.54–1.47 (m, 2H), 0.78–0.69 (m, 1H), 0.48–0.42 (m, 2H), 0.11–0.05 (m, 2H).

***N*-(2-Cyclopropylethyl)-6-(4-(2-(dimethylamino)benzoyl)piperazin-1-yl)pyridazine-3-carboxamide (46).** White solid (61% yield). ¹H NMR (300 MHz, CDCl₃) δ 8.04 (d, *J* = 9.5 Hz, 1H), 7.96 (t, *J* = 5.9 Hz, 1H), 7.36–7.25 (m, 2H), 7.05–6.94 (m, 3H), 4.17–4.05 (m, 1H), 3.98–3.72 (m, 5H), 3.60–3.43 (m, 3H), 3.37–3.24 (m, 1H), 2.80 (s, 6H), 1.53–1.49 (m, 2H), 0.80–0.73 (m, 1H), 0.47–0.42 (m, 2H), 0.12–0.07 (m, 2H).

6-(4-(2-Chloro-5-(dimethylamino)benzoyl)piperazin-1-yl)-*N*-(2-cyclopropylethyl)pyridazine-3-carboxamide (47). White solid (53% yield). ¹H NMR (300 MHz, CDCl₃) δ 8.04 (d, *J* = 9.6 Hz, 1H), 7.96 (t, *J* = 5.8 Hz, 1H), 7.39 (d, *J* = 9.0 Hz, 1H), 6.94 (d, *J* = 9.6 Hz, 1H), 6.66 (dd, *J* = 9.0, 3.0 Hz, 1H), 6.55 (d, *J* = 3.0 Hz, 1H), 4.14–4.00 (m, 1H), 3.92–3.71 (m, 5H), 3.58–3.32 (m, 4H), 2.93 (s, 6H), 1.52 (q, *J* = 6.9 Hz, 2H), 0.75–0.69 (m, 1H), 0.48–0.42 (m, 2H), 0.11–0.05 (m, 2H). MS (ES+) *m/z* 457.4 (M + H)⁺.

6-(4-(2-Chloro-5-fluorobenzoyl)piperazin-1-yl)-*N*-(2-cyclopropylethyl)pyridazine-3-carboxamide (48). White solid (94% yield); mp 194–196 °C. ¹H NMR (300 MHz, CDCl₃) δ 8.05 (d, *J* = 9.4 Hz, 1H), 7.96 (t, *J* = 6.0 Hz, 1H), 7.41–7.37 (m, 1H), 7.11–7.03 (m, 2H), 7.00 (d, *J* = 9.4 Hz, 1H), 4.07–3.70 (m, 6H), 3.53–3.34 (m, 4H), 1.55–1.46 (m, 2H), 0.79–0.68 (m, 1H), 0.48–0.42 (m, 2H), 0.11–0.06 (m, 2H). MS (ES+) *m/z* 432.2 (M + H)⁺.

***N*-(2-Cyclopropylethyl)-6-(4-(5-fluoro-2-(trifluoromethyl)benzoyl)piperazin-1-yl)pyridazine-3-carboxamide (49).** White solid (65% yield); mp 177–179 °C. ¹H NMR (300 MHz, CDCl₃) δ 8.05 (d, *J* = 9.6 Hz, 1H), 7.97 (t, *J* = 5.7 Hz, 1H), 7.77–7.72 (m, 1H), 7.26–7.2 (m, 1H), 7.08–7.05 (m, 1H), 6.99 (d, *J* = 9.3 Hz, 1H), 4.05–3.99 (m, 1H), 3.89–3.69 (m, 5H), 3.58–3.51 (m, 2H), 3.35 (t, *J* = 5.1 Hz, 2H), 1.53–1.46 (m, 2H), 0.76–0.69 (m, 1H), 0.48–0.42 (m, 2H), 0.10–0.05 (m, 2H). MS (ES+) *m/z* 466.5 (M + H)⁺.

***N*-(2-Cyclopropylethyl)-6-(4-(5-fluoro-2-methoxybenzoyl)piperazin-1-yl)pyridazine-3-carboxamide (50).** White solid (61% yield). ¹H NMR (300 MHz, CDCl₃) δ 8.03 (d, *J* = 9.5 Hz, 1H), 7.96 (t, *J* = 5.9 Hz, 1H), 7.10–6.98 (m, 3H), 6.86–6.84 (m, 1H), 4.03–3.98 (m, 1H), 3.92–3.75 (m, 10H), 3.53–3.37 (m, 2H), 1.53–1.49 (m, 2H), 0.80–0.72 (m, 1H), 0.49–0.44 (m, 2H), 0.15–0.10 (m, 2H). MS (ES+) *m/z* 428.1 (M + H)⁺.

6-(4-(5-Chloro-2-(trifluoromethyl)benzoyl)piperazin-1-yl)-*N*-(2-cyclopropylethyl)pyridazine-3-carboxamide (51). White solid (58% yield). mp 164–166 °C. ¹H NMR (300 MHz, CDCl₃) δ 8.07 (d, *J* = 9.3 Hz, 1H), 7.96 (t, *J* = 5.8 Hz, 1H), 7.69 (d, *J* = 7.8 Hz, 1H), 7.54 (d, *J* = 7.6 Hz, 1H), 7.02 (d, *J* = 9.3 Hz, 1H), 4.07–4.00 (m, 1H), 3.87–3.72 (m, 5H), 3.66–3.60 (m, 2H), 3.42–3.35 (m, 2H), 1.54–1.50 (m, 2H), 0.79–0.68 (m, 1H), 0.48–0.43 (m, 2H), 0.14–0.08 (m, 2H). MS (ES+) *m/z* 482.1 (M + H)⁺.

***N*-(2-Cyclopropylethyl)-6-(4-(2,5-dimethylbenzoyl)piperazin-1-yl)pyridazine-3-carboxamide (52).** White solid (56% yield). ¹H NMR (300 MHz, CDCl₃) δ 8.05 (d, *J* = 9.6 Hz, 1H), 7.96 (t, *J* = 5.8 Hz, 1H), 7.16–7.11 (m, 2H), 7.03–6.97 (m, 2H), 4.12–3.65 (m, 6H), 3.60–3.54 (m, 2H), 3.43–3.38 (m, 2H), 2.23 (s, 3H),

2.22 (s, 3H), 1.54–1.50 (m, 2H), 0.82–0.69 (m, 1H), 0.48–0.42 (m, 2H), 0.11–0.05 (m, 2H). MS (ES+) m/z 408.3 (M + H)⁺.

N-(2-Cyclopropylethyl)-6-(4-(2,5-difluorobenzoyl)piperazin-1-yl)pyridazine-3-carboxamide (53). White solid (53% yield). ¹H NMR (400 MHz, CDCl₃) δ 8.08 (d, J = 7.6 Hz, 1H), 8.00 (t, J = 5.7 Hz, 1H), 7.17–7.11 (m, 3H), 7.03 (d, J = 7.6 Hz, 1H), 4.02–3.92 (m, 2H), 3.85–3.83 (m, 4H), 3.59–3.5 (m, 4H), 1.54–1.50 (m, 2H), 0.74–0.69 (m, 1H), 0.46–0.40 (m, 2H), 0.09–0.04 (m, 2H).

N-(2-Cyclopropylethyl)-6-(4-(2,5-dichlorobenzoyl)piperazin-1-yl)pyridazine-3-carboxamide (54). White solid (54% yield). ¹H NMR (300 MHz, CDCl₃) δ 8.05 (d, J = 9.6 Hz, 1H), 7.96 (t, J = 5.8 Hz, 1H), 7.38–7.30 (m, 3H), 6.97 (d, J = 9.6 Hz, 1H), 4.12–3.70 (m, 6H), 3.60–3.23 (m, 4H), 1.54–1.50 (m, 2H), 0.80–0.67 (m, 1H), 0.51–0.38 (m, 2H), 0.16–0.06 (m, 2H). MS (ES+) m/z 448.2 (M + H)⁺.

6-(4-(2,5-Bis(trifluoromethyl)benzoyl)piperazin-1-yl)-N-(2-cyclopropylethyl)pyridazine-3-carboxamide (55). White solid (50% yield). ¹H NMR (400 MHz, CDCl₃) δ 8.08 (d, J = 7.6 Hz, 1H), 7.99 (t, J = 5.7 Hz, 1H), 7.92–7.90 (m, 1H), 7.85–7.84 (m, 1H), 7.65 (s, 1H), 7.02 (d, J = 7.6 Hz, 1H), 4.13–4.08 (m, 1H), 3.95–3.71 (m, 5H), 3.57–3.55 (m, 2H), 3.38–3.36 (m, 2H), 1.57–1.44 (m, 2H), 0.8–0.7 (m, 1H), 0.48–0.46 (m, 2H), 0.16–0.08 (m, 2H).

N-(2-Cyclopropylethyl)-6-(4-(3-fluoro-2-(trifluoromethyl)benzoyl)piperazin-1-yl)pyridazine-3-carboxamide (56). White solid (31% yield). ¹H NMR (300 MHz, CDCl₃) δ 8.05 (d, J = 9.6 Hz, 1H), 7.97 (t, J = 5.7 Hz, 1H), 7.65–7.59 (m, 1H), 7.29 (d, J = 9.6 Hz, 1H), 7.12 (d, J = 7.8 Hz, 1H), 6.99 (d, J = 9.6 Hz, 1H), 4.05–3.99 (m, 1H), 3.89–3.72 (m, 5H), 3.54 (q, J = 6.6 Hz, 2H), 3.35 (t, J = 5.1 Hz, 2H), 1.53–1.50 (m, 2H), 0.76–0.71 (m, 1H), 0.48–0.42 (m, 2H), 0.10–0.05 (m, 2H).

N-(2-Cyclopropylethyl)-6-(4-(4-fluoro-2-(trifluoromethyl)benzoyl)piperazin-1-yl)pyridazine-3-carboxamide (57). White solid (83% yield). ¹H NMR (300 MHz, CDCl₃) δ 8.05 (d, J = 9.6 Hz, 1H), 7.97 (t, J = 5.7 Hz, 1H), 7.46–7.42 (m, 1H), 7.39–7.29 (m, 2H), 6.97 (d, J = 9.6 Hz, 1H), 4.07–4.01 (m, 1H), 3.89–3.67 (m, 5H), 3.58–3.51 (m, 2H), 3.36–3.32 (m, 2H), 1.53–1.47 (m, 2H), 0.76–0.69 (m, 1H), 0.48–0.42 (m, 2H), 0.10–0.06 (m, 2H). MS (ES+) m/z 466.1 (M + H)⁺.

N-(2-Cyclopropylethyl)-6-(4-(4,4,4-trifluorobut-2-enoyl)piperazin-1-yl)pyridazine-3-carboxamide (37). To a solution of 4,4,4-trifluorobut-2-enoic acid (62 mg, 0.44 mmol) in DCM (6 mL) was added DIPEA (0.18 mL, 1.03 mmol), followed by the addition of HOBt (68.7 mg, 0.51 mmol) and EDCI (0.10 mL, 0.57 mmol). The resulting mixture was stirred for 15 min, and N-(2-cyclopropylethyl)-6-(piperazin-1-yl)pyridazine-3-carboxamide (0.10 g, 0.36 mmol) was added. After stirring overnight at room temperature, the reaction mixture was diluted with EtOAc (120 mL), washed with water (4 × 12 mL) and brine (2 × 15 mL), dried over anhydrous Na₂SO₄, and concentrated in vacuo. Purification by column chromatography afforded the product as a white solid (28.5 mg, 20% yield). ¹H NMR (500 MHz, CDCl₃) δ 8.09 (d, J = 9.8 Hz, 1H), 8.00 (br s, 1H), 7.02–6.98 (m, 2H), 6.83–6.79 (m, 1H), 3.96–3.88 (m, 4H), 3.80–3.76 (m, 4H), 3.61–3.55 (m, 2H), 1.54–1.51 (m, 2H), 0.78–0.63 (m, 1H), 0.52–0.34 (m, 2H), 0.12–0.02 (m, 2H). MS (ES+) m/z 398.0 (M + H)⁺.

The general procedure described for 37 was followed for the preparation of the following compounds, using the appropriate carboxylic acid for amide formation.

N-(2-Cyclopropylethyl)-6-(4-(2-(trifluoromethyl)cyclopropanecarbonyl)piperazin-1-yl)pyridazine-3-carboxamide (38). White solid (31% yield). ¹H NMR (300 MHz, CDCl₃) δ 8.03 (d, J = 9.6 Hz, 1H), 7.98 (br s, 1H), 7.00 (d, J = 9.6 Hz, 1H), 3.97–3.57 (m, 10H), 2.22–1.98 (m, 1H), 1.67–1.63 (m, 1H), 1.52–1.49 (m, 2H), 1.28–1.24 (m, 2H), 0.77–0.73 (m, 1H), 0.48–0.44 (m, 2H), 0.011–0.08 (m, 2H). MS (ES+) m/z 412.0 (M + H)⁺.

N-(2-Cyclopropylethyl)-6-(4-(2-methylcyclohexanecarbonyl)piperazin-1-yl)pyridazine-3-carboxamide (39). White solid (60% yield). ¹H NMR (300 MHz, CDCl₃) δ 8.08 (d, J = 9.6 Hz, 1H), 8.00 (t, J = 5.7 Hz, 1H), 7.00 (d, J = 9.3 Hz, 1H), 3.98–3.60 (m, 10H), 2.75–2.68 (m, 1H), 2.05–1.98 (m, 1H), 1.90–1.42 (m, 9H), 1.26–1.24 (m, 1H), 0.95 (d, J = 6.6 Hz, 3H), 0.80–0.72 (m, 1H),

0.50–0.45 (m, 2H), 0.15–0.05 (m, 2H). MS (ES+) m/z 400.0 (M + H)⁺.

N-(2-Cyclopropylethyl)-6-(4-(2-(trifluoromethyl)furan-3-carbonyl)piperazin-1-yl)pyridazine-3-carboxamide (40). White solid (71% yield). ¹H NMR (300 MHz, CDCl₃) δ 8.04 (d, J = 10.6 Hz, 1H), 7.96 (t, J = 6.0 Hz, 1H), 7.56 (d, J = 6.0 Hz, 1H), 7.00 (d, J = 10.6 Hz, 1H), 6.54 (s, 1H), 3.90–3.70 (m, 6H), 3.60–3.50 (m, 4H), 1.49 (q, J = 7.0 Hz, 2H), 0.79–0.66 (m, 1H), 0.50–0.47–0.41 (m, 2H), 0.09–0.04 (m, 2H). MS (ES+) m/z 438.0 (M + H)⁺.

N-(2-Cyclopropylethyl)-6-(4-(5-methyl-2-(trifluoromethyl)furan-3-carbonyl)piperazin-1-yl)pyridazine-3-carboxamide (42). White solid (53% yield); mp 128–130 °C. ¹H NMR (500 MHz, CDCl₃) δ 8.08 (d, J = 9.5 Hz, 1H), 7.99 (t, J = 5.0 Hz, 1H), 7.01 (d, J = 9.5 Hz, 1H), 6.15 (s, 1H), 3.94–3.89 (m, 2H), 3.82–3.77 (m, 4H), 3.60–3.52 (m, 4H), 2.39 (s, 3H), 1.54–1.50 (m, 2H), 0.80–0.71 (m, 1H), 0.49–0.45 (m, 2H), 0.13–0.08 (m, 2H). MS (ES+) m/z 452.0 (M + H)⁺.

2-(4-(6-((2-Cyclopropylethyl)carbamoyl)pyridazin-3-yl)-piperazine-1-carbonyl)benzoic Acid (44). Step 1: To a solution of monomethyl phthalate (142 mg, 0.78 mmol) in DCM (10 mL) was added DIPEA (0.2 mL, 1.15 mmol), HOBt monohydrate (116 mg, 0.86 mmol), and EDCI (0.16 mL, 1.38 mmol). The resulting mixture was stirred for 15 min, followed by the addition of N-(2-cyclopropylethyl)-6-(piperazin-1-yl)pyridazine-3-carboxamide (184 mg, 0.66 mmol). The reaction mixture was stirred for 18 h and diluted with ethyl acetate (100 mL), washed with water and brine, dried over anhydrous Na₂SO₄, and concentrated. Purification by flash chromatography (ethyl acetate) and recrystallization from ethyl acetate and hexanes afforded methyl 2-(4-(6-((2-cyclopropylethyl)-carbamoyl)pyridazin-3-yl)piperazine-1-carbonyl)benzoate as a white solid (241 mg, 83% yield). MS (ES+) m/z 438.1 (M + H)⁺.

Step 2: LiOH·H₂O (66 mg, 1.57 mmol) was added to a solution of methyl 2-(4-(6-((2-cyclopropyl-ethyl)carbamoyl)pyridazin-3-yl)-piperazine-1-carbonyl)benzoate (230 mg, 0.52 mmol) in THF (10 mL) and water (5 mL). The reaction mixture was stirred at room temperature overnight. THF was removed in vacuo. The residue was dissolved in ethyl acetate (100 mL) and neutralized by the addition of 5% HCl solution, washed with brine, dried over anhydrous Na₂SO₄, and concentrated. The residue was recrystallized from dichloromethane and hexanes to afford 44 as a white solid (107 mg, 42% yield). ¹H NMR (300 MHz, CDCl₃) δ 8.67 (br s, 1H), 9.07–7.87 (m, 3H), 7.54 (t, J = 7.5 Hz, 1H), 7.41 (t, J = 7.5 Hz, 1H), 7.26–7.24 (m, 1H), 6.95 (d, J = 9.6 Hz, 1H), 4.12–3.67 (m, 6H), 3.56–3.42 (m, 2H), 3.38–3.27 (m, 2H), 1.55–1.40 (m, 2H), 0.77–0.64 (m, 1H), 0.50–0.34 (m, 2H), 0.13–0.01 (m, 2H). MS (ES+) m/z 424.2 (M + H)⁺.

Preparation of Mouse Liver Microsomes. Male ICR mice, on a high-carbohydrate, low-fat diet, under light halothane (15% in mineral oil) anesthesia were sacrificed by exsanguination during periods of high enzyme activity. Livers were immediately rinsed with cold 0.9% NaCl solution, weighed, and minced with scissors. All procedures were performed at 4 °C unless specified otherwise. Livers were homogenized in a solution (1:3 w/v) containing 0.25 M sucrose, 62 mM potassium phosphate buffer (pH 7.0), 0.15 M KCl, 1.5 mM N-acetylcysteine, 5 mM MgCl₂, and 0.1 mM EDTA using four strokes of a Potter–Elvehjem tissue homogenizer. The homogenate was centrifuged at 10400g for 20 min to eliminate mitochondria and cellular debris. The supernatant was filtered through a three-layer cheesecloth and centrifuged at 105000g for 60 min. The microsomal pellet was gently resuspended in the same homogenization solution, and the protein concentration was measured using bovine serum albumin as the standard.

SCD1 Mouse Liver Microsomal Activity Assay. Assay methodology is based on the method first described by Talamo and Bloch.³⁸ SCD1 activity was measured using radiolabeled substrate, [9,10-³H]-stearoyl-Coenzyme A, for conversion into oleoyl-Coenzyme A and release of tritiated water. Reactions were initiated by the addition of 60 μ g of microsomal protein to assay plates containing 0.20 μ Ci of the substrate at a final concentration of 33 μ M with 2.0 mM NADH in a 33 mM Na-phosphate buffer (pH 7.4). Plates were incubated for 20

min at 25 °C, and the reactions were stopped using 10 μ L of 60% perchloric acid. Reactions were transferred to multiscreen filter plates coated with 0.5% charcoal to bind the unreacted labeled substrate, and the released tritiated water was collected and counted in a Microscint 40 scintillation counter.

Cell-Based SCD1 Activity Assay. The method was based on the published procedure by Obukowicz.³⁹ Human liver hepatocellular carcinoma cells (HepG2) were grown to 50–60% confluency and washed with phosphate-buffered saline prior to incubation with test compounds and radiolabeled stearic acid (15 μ Ci) for 24 h at 37 °C. The cells were treated with 5N NaOH to saponify the substrate and product fatty acids. Fatty acids were extracted with hexane and separated by thin layer chromatography. Plates were read on an instant imager to detect the substrate and product, and the percent conversion was determined. The effect of the test compounds on SCD1 activity, as assessed by the conversion of radiolabeled stearic acid (18:0) into oleic acid (*cis*-9-octadecenoic acid 18:1-n9), was evaluated against a control to determine the percent of residual activity.

Plasma Desaturation Index (DI) Determination. Plasma lipids were extracted following a modified Folch procedure, and the different lipid classes contained in the extract were separated by thin layer chromatography. The desired lipid classes were hydrolyzed to form free fatty acids, which were subsequently derivatized for analysis by gas chromatography. GC analysis was performed to provide a profile of the amounts of the individual fatty acids contained in the lipid fraction. The quantitative amount of each individual fatty acid was determined by comparison to a known amount of internal standard added at the extraction stage. The plasma DI was calculated based on the ratio of substrate and product as described.⁹

Delta-5 and delta-6 Desaturase Activity. This method was based on the procedure reported by Obukowicz.³⁹ Microsomes for the measurement of delta-5 and delta-6 desaturase activity were prepared as described above. Delta-6 desaturase activity was measured using radiolabeled linoleic acid (*cis,cis*-9,12-octadecadienoic acid, 18:2-n6) as a substrate for conversion into γ -linolenic acid (all *cis*-6,9,12-octadecatrienoic acid, 18:3-n6). Thin layer chromatography was then used to separate the substrate and product following saponification and extraction of fatty acids as described above. The effects of the test compounds on delta-5 and delta-6 desaturase activities were evaluated against a solvent control to determine the percent of residual activity.

Efficacy Study in Zucker Fatty Rats. Twenty-week-old male Zucker obese fa/fa rats purchased from Harlan Sprague–Dawley Inc. (Indianapolis, Indiana) were quarantined for approximately one week. Two rats were housed per cage in a separate, controlled room. Temperature was between 18 and 25 °C and relative humidity between 45 and 65%. There was a 12 h light/dark cycle and rats had access to filtered tap water and rodent Teklad 2018 diet was fed ad libitum throughout the study unless specified. After quarantine period, rats were randomly divided into two groups of 24 rats each with equivalent average total body weights. These two groups were randomly assigned to 49 treatment group (1 mg/kg) or vehicle control group. 49 was suspended in a mixture of 1% CMC (low viscosity), 0.1% Tween 20, 10% propylene glycol, and 88.9% water. Rats were administered orally twice a day at 10 a.m. and 4 p.m., respectively, for 15 weeks. The body weight was measured each day for each rat. At the end of the 15 weeks of treatment, the rats were fasted for 4 h and received the final dose of 49 or vehicle 2 h prior to being euthanized by exsanguination. Following termination, dual energy X-ray absorptiometry (DEXA) measurement of bone mineral content (BMC), lean mass, and fat mass in the thoracovisceral area of the carcasses was measured.

Body Weight. When the rat was motionless on the weighing apparatus, the total body weight was measured for each rat following the 10 a.m. dosing each day.

Visceral Adipose Tissue Weight. Following termination, carcasses were kept at 4 °C overnight. Epididymal, mesenteric, and retroperitoneal fat pads were dissected and weighed.

DEXA Measurement. Following termination, dual energy X-ray absorptiometry (DEXA) measurement of bone mineral content (BMC), lean mass, and fat mass in the thoracovisceral area of the

carcasses was carried out with a Norland pDEXA machine equipped with Sabre small animal analysis software (Orthometrics).

AUTHOR INFORMATION

Corresponding Author

*Phone: 604-484-3361. E-mail: mwinther@xenon-pharma.com.

Notes

The authors declare no competing financial interest.

ACKNOWLEDGMENTS

We thank our colleagues at Xenon Pharmaceuticals, Inc., who assisted in the technical conduct of the research, including: Catherine Zaborowska, Mary Huber, Maryann Mattice, Chris Radomski, Joseph Sanghara, Pritpaul Samra, Rainbow Kwan, Ivana Rajlic, Darren Daley, Caroline Hall, Audrey Wang, Annick Legendre, Robert Fraser, and Monica Mork. We also thank our colleagues at the former Discovery Partners International, ChemRx Division, Wenbao Li, Mikhail Kondratenko, Chi Tu, Melwyn Abreo, and Mark W. Holladay, and at Novartis AG, Natalie Dales, Bryan Burkey, Andreas Billich, and Brian Hubbard.

ABBREVIATIONS USED

SCD1, stearoyl coenzyme A desaturase 1; C16:1, palmitoleic acid; C16:0, palmitic acid; C18:1, oleic acid; C18:0, stearic acid; HepG2, human hepatocellular carcinoma cell line; ip, intraperitoneal; SAR, structure–activity relationship; DI, desaturation index; AUC, area under the curve; ¹H NMR, proton nuclear magnetic resonance; PBS, phosphate buffer solution; ND, not determined; DEXA, dual energy X-ray absorptiometry

REFERENCES

- (1) (a) Kusunoki, J.; Kanatani, A.; Moller, D. E. Modulation of fatty acids metabolism as a potential approach to the treatment of obesity and metabolic syndrome. *Endocrine* **2006**, 29 (1), 91–100. (b) Chavez, J. A.; Summers, S. A. Lipid oversupply, selective insulin resistance, and lipotoxicity: molecular mechanisms. *Biochim. Biophys. Acta* **2010**, 18 (1), 252–265.
- (2) Enoch, H. G.; Catala, A.; Strittmatter, P. Mechanism of rat liver microsomal stearoyl-CoA desaturase. *J. Biol. Chem.* **1976**, 251 (16), 5095–5103.
- (3) Ntambi, J. M. The regulation of stearoyl-CoA desaturase (SCD). *Prog. Lipid Res.* **1995**, 34, 139–150.
- (4) Cohen, P.; Miyazaki, M.; Socci, N. D.; Hagge-Greenberg, A.; Liedtke, W.; Soukas, A. A.; Sharma, R.; Hudgins, L. C.; Ntambi, J. M.; Friedman, J. M. Role for stearoyl-CoA desaturase-1 in leptin-mediated weight loss. *Science* **2002**, 297, 240–243.
- (5) Ntambi, J. M.; Miyazaki, M.; Stoeckel, J. P.; Lan, H.; Kendziorski, C. M.; Yandell, B. S.; Song, Y.; Cohn, P.; Friedman, J. M.; Attie, A. D. Loss of stearoyl-CoA desaturase-1 function protects mice against adiposity. *Proc. Natl. Acad. Sci. U. S. A.* **2002**, 99, 11482–11486.
- (6) Dobrzyn, P.; Sampath, H.; Dobrzyn, A.; Miyazaki, M.; Ntambi, J. M. Loss of stearoyl-CoA desaturase 1 inhibits fatty acid oxidation and increases glucose utilization in the heart. *Am. J. Physiol.: Endocrinol. Metab.* **2008**, 294, E357–E364.
- (7) Jiang, G.; Li, Z.; Liu, F.; Ellsworth, K.; Dallas-Yang, Q.; Wu, M.; Ronan, J.; Esau, C.; Murphy, C.; Szalkowski, D.; Bergeron, R.; Doebber, T.; Zhang, B. B. Prevention of obesity in mice by antisense oligonucleotide inhibitors of stearoyl-CoA desaturase-1. *J. Clin. Invest.* **2005**, 115, 1030–1038.
- (8) Gutierrez-Juarez, R.; Pocai, A.; Mulas, C.; Ono, H.; Bhanot, S.; Monia, B. P.; Rossetti, L. Critical role of stearoyl-CoA desaturase-1 (SCD1) in the onset of diet-induced hepatic insulin resistance. *J. Clin. Invest.* **2006**, 116, 1686–1695.

- (9) Attie, A. D.; Krauss, R. M.; Gray-Keller, M. P.; Brownlie, A.; Miyazaki, M.; Kastelein, J. J.; Lusis, A. J.; Stalenhoef, A. F.; Stoehr, J. P.; Hayden, M. R.; Ntambi, J. M. Relationship between stearoyl-CoA desaturase activity and plasma triglycerides in human and mouse hypertriglyceridemia. *J. Lipid Res.* **2002**, *43*, 1899–1907.
- (10) Hulver, M. W.; Berggren, J. R.; Carper, M. J.; Miyazaki, M.; Ntambi, J. M.; Hoffman, E. P.; Thyfault, J. P.; Stevens, R.; Dohm, G. L.; Houmard, J. A.; Muoio, D. M. Elevated stearoyl-CoA desaturase-1 expression in skeletal muscle contributes to abnormal fatty acid partitioning in obese humans. *Cell Metab.* **2005**, *2*, 251–261.
- (11) Warensjö, E.; Ingelsson, E.; Lundmark, P.; Lannfelt, L.; Syvänen, L.-C.; Vessby, B.; Risérus, U. Polymorphisms in the SCD1 gene: associations with body fat distribution and insulin sensitivity. *Obesity* **2007**, *15*, 1732–1740.
- (12) Gschwend, H. W.; Kodumuru, V.; Liu, S.; Kamboj, R. Pyridazine derivatives and their use as therapeutic agents. WO 2005/011653 A2, February 10, 2005.
- (13) Abreo, M.; Harvey, D. F.; Kondratenko, M. A.; Li, W.; Kamboj, R.; Kodumuru, V.; Winther, M. D.; Gschwend, H. W.; Chakka, N.; Liu, S.; Sviridov, S.; Sun, S. Pyridyl derivatives and their use as therapeutic agents. WO 2005/011654 A2, February 10, 2005.
- (14) Abreo, M.; Chafeev, M.; Chakka, N.; Chowdhury, S.; Fu, J.; Gschwend, H. W.; Holladay, M. W.; Hou, D.; Kamboj, R.; Kodumuru, V.; Li, W.; Liu, S.; Raina, V.; Sun, S.; Sun, S.; Sviridov, S.; Tu, C.; Winther, M. D.; Zhang, Z. Pyridazine derivatives and their use as therapeutic agents. WO 2005/011655 A2, February 10, 2005.
- (15) Abreo, M.; Harvey, D. F.; Gschwend, H. W.; Li, W.; Tu, C.; Kamboj, R.; Winther, M. D.; Kodumuru, V.; Hudson, C. J.; Kondratenko, M. A.; Liu, S.; Raina, V.; Sviridov, S.; Zhang, Z.; Seid, B. M.; Sun, S. Pyridyl derivatives and their use as therapeutic agents. WO 2005/011656 A2, February 10, 2005.
- (16) Sviridov, S.; Kodumuru, V.; Liu, S.; Abreo, M.; Winther, M. D.; Gschwend, H. W.; Kamboj, R.; Sun, S.; Holladay, M. W.; Li, W.; Tu, C. Piperazine derivatives and their use as therapeutic agents. WO 2005/011657 A2, February 10, 2005.
- (17) Liu, G.; Lynch, J. K.; Freeman, J.; Liu, B.; Xin, Z.; Zhao, H.; Serby, M. D.; Kym, P. R.; Suhar, T. S.; Smith, H. T.; Cao, N.; Yang, R.; Janis, R. S.; Krauser, J. A.; Cepa, S. P.; Beno, D. W. A.; Sham, H. L.; Collins, C. A.; Surowy, T. K.; Camp, H. S. Discovery of potent, selective, orally bioavailable stearoyl-CoA desaturase 1 inhibitors. *J. Med. Chem.* **2007**, *50*, 3086–3100.
- (18) Zhao, H.; Serby, M. D.; Smith, H. T.; Cao, N.; Suhar, T. S.; Surowy, T. K.; Camp, H. S.; Collins, C. A.; Sham, H. L.; Liu, G. Discovery of 1-(4-phenoxy-piperidin-1-yl)-2-arylaminoethanone stearoyl-CoA desaturase 1 inhibitors. *Bioorg. Med. Chem. Lett.* **2007**, *17*, 3388–3391.
- (19) Koltun, D. O.; Parkhill, E. Q.; Vasilevich, N. I.; Glushkov, A. I.; Zilbershtein, T. M.; Ivanov, A. V.; Cole, A. G.; Henderson, I.; Zautke, N. A.; Brunn, S. A.; Mollova, N.; Leung, K.; Chisholm, J. W.; Zabolocki, J. Novel, potent, selective, and metabolically stable stearoyl-CoA desaturase (SCD) inhibitors. *Bioorg. Med. Chem. Lett.* **2009**, *19*, 2048–2052.
- (20) Liu, G. Stearoyl-CoA desaturase inhibitors: update on patented compounds. *Expert Opin. Ther. Pat.* **2009**, *19*, 1169–1191 and references therein.
- (21) Koltun, D. O.; Vasilevich, N. I.; Parkhill, E. Q.; Glushkov, A. I.; Zilbershtein, T. M.; Mayboroda, E. I.; Boze, M. A.; Cole, A. G.; Henderson, I.; Zautke, N. A.; Brunn, S. A.; Chu, N.; Hao, J.; Mollova, N.; Leung, K.; Chisholm, J. W.; Zabolocki, J. Orally bioavailable, liver-selective stearoyl-CoA desaturase (SCD) inhibitors. *Bioorg. Med. Chem. Lett.* **2009**, *19*, 3050–3053.
- (22) Koltun, D. O.; Zilbershtein, T. M.; Migulin, V. A.; Vasilevich, N. I.; Parkhill, E. Q.; Glushkov, A. I.; McGregor, M. J.; Brunn, S. A.; Chu, N.; Hao, J.; Mollova, N.; Leung, K.; Chisholm, J. W.; Zabolocki, J. Potent, orally bioavailable, liver-selective stearoyl-CoA desaturase (SCD) inhibitors. *Bioorg. Med. Chem. Lett.* **2009**, *19*, 4070–4074.
- (23) Uto, Y.; Ueno, Y.; Kiyotsuka, Y.; Miyazawa, Y.; Kurata, H.; Ogata, T.; Yamada, M.; Deguchi, T.; Konishi, M.; Tekagi, T.; Wakimoto, S.; Ohsumi, J. Synthesis and evaluation of novel stearoyl-CoA desaturase 1 inhibitors: 1'-{6-[5-(pyridin-3-ylmethyl)-1,3,4-oxadiazol-2-yl]pyridazin-3-yl}-3,4-dihydro-spiro[chromene-2,4'-piperidine] analogs. *Eur. J. Med. Chem.* **2010**, *45*, 4788–4796.
- (24) Ramtohl, Y. K.; Black, C.; Chan, C.; Crane, S.; Guay, J.; Guiral, S.; Huang, Z.; Oballa, R.; Xu, L.; Zhang, L.; Li, C. S. SAR and optimization of thiazole analogs as potent stearoyl-CoA desaturase inhibitors. *Bioorg. Med. Chem. Lett.* **2010**, *20*, 1593–1597.
- (25) Atkinson, K. A.; Beretta, E. E.; Brown, J. A.; Castrodad, M.; Chen, Y.; Cosgrove, J. M.; Du, P.; Litchfield, J.; Makowski, M.; Martin, K.; McLellan, T. J.; Neagu, C.; Perry, D. A.; Piotrowski, D. W.; Stepan, C. M.; Trilles, R. N-Benzylimidazole carboxamides as potent, orally active stearoyl CoA desaturase-1 inhibitors. *Bioorg. Med. Chem. Lett.* **2010**, *21*, 1621–1625.
- (26) Uto, Y.; Ueno, Y.; Kiyotsuka, Y.; Miyazawa, Y.; Kurata, H.; Ogata, T.; Takagi, T.; Wakimoto, S.; Ohsumi, J. Discovery of novel SCD1 inhibitors: 5-Alkyl-4,5-dihydro-3H-spiro[1,5-benzoxazepine-2,40-piperidine] analogs. *Eur. J. Med. Chem.* **2011**, *46*, 1892–1896.
- (27) Oballa, R. M.; Belair, L. W.; Black, C.; Bleasby, K.; Chan, C. C.; Desroches, C.; Du, X.; Gordon, R.; Guay, J.; Guiral, S.; Hafey, M. J.; Hamelin, E.; Huang, Z.; Kennedy, B.; Lachance, N.; Landry, F.; Li, C. S.; Mancini, J.; Normandin, D.; Poci, A.; Powell, D. A.; Ramtohl, Y. K.; Skorey, K.; Sørensen, D.; Sturkenboom, W.; Styhler, A.; Waddleton, D. M.; Wang, H.; Wong, S.; Xu, L.; Zhang, L. Development of a liver-targeted stearoyl-CoA desaturase (SCD) inhibitor (MK-8245) to establish a therapeutic window for the treatment of diabetes and dyslipidemia. *J. Med. Chem.* **2011**, *54*, 5082–5096.
- (28) Leclerc, J. P.; Falgout, J. P.; Girardin, M.; Guay, J.; Guiral, S.; Huang, Z.; Li, C. S.; Oballa, R.; Ramtohl, Y. K.; Skorey, K.; Tawa, P.; Wang, H.; Zhang, L. Conversion of systemically-distributed triazole-based stearoyl-CoA desaturase (SCD) uHTS hits into liver-targeted SCD inhibitors. *Bioorg. Med. Chem. Lett.* **2011**, *21*, 6505–6509.
- (29) Powell, D. A.; Black, W. C.; Bleasby, K.; Chan, C. C.; Deschenes, D.; Gagnon, M.; Gordon, R.; Guay, J.; Guiral, S.; Hafey, M. J.; Huang, Z.; Isabel, E.; Leblanc, Y.; Styhler, A.; Xu, L. J.; Zhang, L.; Oballa, R. M. Nicotinic acids: Liver-targeted SCD inhibitors with preclinical anti-diabetic efficacy. *Bioorg. Med. Chem. Lett.* **2011**, *21*, 7281–7286.
- (30) Lachance, N.; Guiral, S.; Huang, Z.; Leclerc, J. P.; Li, C. S.; Oballa, R. M.; Ramtohl, Y. K.; Wang, H.; Wu, J.; Zhang, L. Discovery of potent and liver-selective stearoyl-CoA desaturase (SCD) inhibitors in an acyclic linker series. *Bioorg. Med. Chem. Lett.* **2012**, *22*, 623–627.
- (31) Lachance, N.; Gareau, Y.; Guiral, S.; Huang, Z.; Isabel, E.; Leclerc, J. P.; Léger, S.; Martins, E.; Nadeau, C.; Oballa, R. M.; Ouellet, S. G.; Powell, D. A.; Ramtohl, Y. K.; Tranmer, G. K.; Trinh, T.; Wang, H.; Zhang, L. Discovery of potent and liver-targeted stearoyl-CoA desaturase (SCD) inhibitors in a bispyrrolidine series. *Bioorg. Med. Chem. Lett.* **2012**, *22*, 980–984.
- (32) Fu, J. M.; Kodumuru, V.; Sun, S.; Winther, M. D.; Fine, R. M.; Harvey, D. F.; Klebansky, B.; Gray-Keller, M. P.; Gschwend, H. W.; Li, W. Nicotinamide derivatives and their use as therapeutic agents. US 2005/0119251 A1, June 2, 2005.
- (33) Gray-Keller, M. P.; Winther, M. D.; Fine, R. M.; Klebansky, B.; Gschwend, H.; Harvey, D. F. Pyridylpiperazines and aminonicotinamides and their use as therapeutic agents. US 7,390,813 B1, June 24, 2008.
- (34) Murahashi, S.; Naota, T.; Saito, E. Ruthenium-Catalyzed Amidation of Nitriles with Amines. A Novel, Facile Route to Amides and Polyamides. *J. Am. Chem. Soc.* **1986**, *108*, 7846–7847.
- (35) Nivikoff, P. M. Fatty liver induced in Zucker “fatty” (ff) rats by a semisynthetic diet rich in sucrose. *Proc. Natl. Acad. Sci. U. S. A.* **1977**, *74*, 3038–3042.
- (36) Kurtz, T. W.; Morris, R. C.; Pershadsingh, H. A. The Zucker fatty rat as a genetic model of obesity and hypertension. *Hypertension* **1989**, *13*, 896–901.
- (37) Janusz, J. M.; Young, P. A.; Ridgeway, J. M.; Scherz, M. W.; Enzweiler, K.; Wu, L. I.; Gan, L.; Chen, J.; Kellstein, D. E.; Green, S. A.; Tulich, J. L.; Rosario-Jansen, T.; Magrisso, I. J.; Wehmeyer, K. R.; Kuhlbeck, D. L.; Eichhold, T. H.; Dobson, R. L. M. New

cyclooxygenase-2/5-lipoxygenase inhibitors. 3. 7-*tert*-Butyl-2,3-dihydro-3,3-dimethylbenzofuran derivatives as gastrointestinal safe antiinflammatory and analgesic agents: variations at the 5 position. *J. Med. Chem.* **1998**, *41*, 3515–3529.

(38) Talamo, B. R.; Bloch, K. A new assay for fatty acid desaturation. *Anal. Biochem.* **1969**, *29*, 300–304.

(39) Obukowicz, M. G.; Raz, A.; Pyla, P. D.; Rico, J. G.; Wendling, J. M.; Needleman, P. Identification and characterization of a novel $\Delta 6/\Delta 5$ fatty acid desaturase inhibitor as a potential anti-inflammatory agent. *Biochem. Pharmacol.* **1998**, *55*, 1045–1058.